



Neuroscience and Biobehavioral Reviews

journal homepage: www.elsevier.com/locate/neubiorev

Review

Test-retest reliabilities of resting-state fMRI measurements in human brain functional connectomics: A systems neuroscience perspective

Xi-Nian Zuo ^{a,b,c,*}, Xiu-Xia Xing ^{d,**}^a Key Laboratory of Behavioral Science, Institute of Psychology, Chinese Academy of Sciences, Beijing 100101, China^b Laboratory for Functional Connectome and Development, Institute of Psychology, Chinese Academy of Sciences, Beijing 100101, China^c Magnetic Resonance Imaging Research Center, Institute of Psychology, Chinese Academy of Sciences, Beijing 100101, China^d College of Applied Sciences, Beijing University of Technology, Beijing 100124, China

ARTICLE INFO

Article history:

Received 17 February 2014

Received in revised form 12 May 2014

Accepted 15 May 2014

Available online 27 May 2014

Keywords:

Test-retest reliability

Reproducibility

Resting state fMRI

Brain connectome

Functional connectomics

ABSTRACT

Resting-state functional magnetic resonance imaging (RFMRI) enables researchers to monitor fluctuations in the spontaneous brain activities of thousands of regions in the human brain simultaneously, representing a popular tool for macro-scale functional connectomics to characterize normal brain function, mind-brain associations, and the various disorders. However, the test-retest reliability of RFMRI remains largely unknown. We review previously published papers on the test-retest reliability of voxel-wise metrics and conduct a meta-summary reliability analysis of seven common brain networks. This analysis revealed that the heteromodal associative (default, control, and attention) networks were mostly reliable across the seven networks. Regarding examined metrics, independent component analysis with dual regression, local functional homogeneity and functional homotopic connectivity were the three mostly reliable RFMRI metrics. These observations can guide the use of reliable metrics and further improvement of test-retest reliability for other metrics in functional connectomics. We discuss the main issues with low reliability related to sub-optimal design and the choice of data processing options. Future research should use large-sample test-retest data to rectify both the within-subject and between-subject variability of RFMRI measurements and accelerate the application of functional connectomics.

© 2014 Elsevier Ltd. All rights reserved.

Contents

1. Introduction	101
2. Functional metrics of brain connectomes with RFMRI	102
2.1. The regional characteristics of a single voxel	103
2.2. The relational characteristics among multiple voxels	103
2.3. Computational platforms and big data sharing	104
3. Test-retest reliability in functional connectomics	105
3.1. The concept of test-retest reliability	105
3.2. The need for biomarkers and correction for attenuation	106
3.3. Test-retest reliability of functional connectome metrics	106
4. Further considerations and future directions	109
4.1. Factors interfering with test-retest reliability	109
4.2. Improving reliability in functional connectomics	111
4.3. Call for consortium for reliability and reproducibility	112

* Corresponding author at: Key Laboratory of Behavioral Science, Institute of Psychology, Chinese Academy of Sciences, Beijing 100101, China. Tel.: +86 1064853798; fax: +86 1064853798.

** Corresponding author at: College of Applied Sciences, Beijing University of Technology, Beijing 100124, China.

E-mail addresses: zuoxn@psych.ac.cn, zuoxinian@gmail.com (X.-N. Zuo), xingxx@bjut.edu.cn (X.-X. Xing).

URL: <http://lfcd.psych.ac.cn> (X.-N. Zuo).

5. Conclusions and recommendations.....	113
Funding.....	114
Conflict of interest statement.....	114
Acknowledgments.....	114
References.....	114

1. Introduction

Connectomics has rapidly become a revolution in basic brain research following the introduction of the key concept of the brain connectome, which conceptualizes the connection of the entire brain at different scales as a complex and dynamic system (Sporns et al., 2005; Sporns, 2013). The macro-scale brain structural connectome has been mapped out as a graph with 50–1000 nodes based on structural magnetic resonance imaging (MRI) (He et al., 2007) or diffusion tensor imaging (DTI) (Hagmann et al., 2008; Gong et al., 2009). Brain dynamics are shaped by the brain connectome structure and topology (Deco et al., 2011; Bullmore and Sporns, 2009, 2012) and can be measured with resting-state functional MRI (RFMRI) with different spatial (millimeters) and temporal (seconds) resolutions (Biswal et al., 1995) as well as use of graph theory (Salvador et al., 2005; Achard et al., 2006). At this macro-scale, the functional connectivity of the entire brain connectome or brain graph (Bullmore and Bassett, 2011) has been termed the ‘functional connectome’ (Biswal et al., 2010; Zuo et al., 2012; Kelly et al., 2012), which, conceptually, is another term for the functional outcomes of the brain connectome.

Over the last two decades, macro-scale functional connectomics (i.e., the functional connectomes revealed with RFMRI) has rapidly become a powerful tool in the study of human brain function and associations with mind, behavior and disease (Craddock et al., 2013; Castellanos et al., 2013). For example, the default mode or default network (DMN) of the human brain represents a remarkable and successful indication of discovery science with functional connectomics (Buckner, 2012). This network originally referred to a set of brain regions including the posterior cingulate, hippocampus, medial prefrontal and inferior parietal cortex, which are functionally connected (Greicius et al., 2003) and reliably deactivates during most externally focused tasks (Shulman et al., 1997) but exhibits elevated metabolism during internal cognitive processes (Raichle et al., 2001). The function of the DMN has been related to episodic memory (Buckner et al., 2005), mind wandering (Mason et al., 2007) and various traits (e.g., Adelstein et al., 2011, personality). Furthermore, DMN alterations have been widely observed in neurodegenerative diseases such as Alzheimer’s disease (AD) (Greicius et al., 2004) and psychiatric disorders (Greicius, 2008; Broyd et al., 2009; Fornito and Bullmore, 2010). Between-group differences or inter-individual variability in functional connectomics have greatly enriched our knowledge of specific cortical areas (e.g., (Leech and Sharp, 2014), the posterior cingulate cortex) and elucidated the meaningful and stable properties of the human brain functional connectivity (Buckner et al., 2013).

Although functional connectomes have demonstrated features that are temporally stable or exhibit statistically ignorable intra-individual variability, the temporal dynamics of these connectomes have recently received substantial attention (Hutchison et al., 2013). There are both neural and non-neural factors that likely contribute to the dynamic changes in resting-state functional connectivity. Although exploratory, emerging evidence suggests that dynamic RSFC patterns indicate the intrinsic functional architecture of the human brain (Deco and Corbetta, 2011) as it relates to normal cognition (Albert et al., 2009; Bassett et al., 2011; Mantzaris et al., 2013), behavior (Fox et al., 2007; Hesselmann et al., 2008; Sadaghiani et al., 2010) and clinical diseases (e.g.,

Jones et al., 2012, AD). Meanwhile, the intra-individual variability of resting-state functional connectivity can be partly attributed to various non-neural factors including scan conditions (Yan et al., 2009), head motion (Power et al., 2012; Van Dijk et al., 2012; Satterthwaite et al., 2012, 2013; Yan et al., 2013a), physiological noise (Birn et al., 2008; Chang et al., 2009; Chang and Glover, 2009a,b), and data analysis/standardization strategies (Yan et al., 2013b). In summary, factors that can affect the intra-individual variability of RSFC patterns raise concerns regarding the test-retest reliabilities of functional metrics of the brain connectome with RFMRI.

High test-retest reliability requires both low intra-individual and high inter-individual variability (Barnhart et al., 2007). Low intra-individual variability indicates a high stability across different points in time, and high inter-individual variability implies highly differentiable measures across subjects. High test-retest reliability is particularly important for the development of biomarker-based clinical tests for early detection, timely interventions and diagnoses of brain disorders, especially psychiatric disorders, which currently lack a gold standard biological definition (Kapur et al., 2012). Surprisingly, however, the importance of test-retest reliability has been overlooked in functional connectomics until several recent studies on the test-retest reliability of RFMRI were published (Shehzad et al., 2009; Zuo et al., 2010a,b). As mentioned, RFMRI offers both high temporal and spatial resolutions to examine whole brain activity *in vivo*. A common spatial unit of RFMRI measurements is called the volumetric element (voxel) of several millimeters. While previous studies on functional connectomes conducted with large-scale parcellation provided great insight into brain network organization (Bullmore and Sporns, 2009, 2012), regional variations in local functional homogeneity (Zang et al., 2004; Zuo et al., 2013) suggested that defining a node based on a large structural region and building an edge between a pair of nodes in a brain graph can be problematic. Simply averaging the voxel-wise time series in a large region ignores the fact that the strength of functional homogeneity within the region is typically low and highly variable across spatial locations (Jiang et al., 2014), leading to difficulties in interpreting the mean time series and derived functional metrics in relation to raw time series. This highlights the importance of voxel-wise assessments on the intrinsic functional architecture.

The present work will survey common voxel-wise metrics used in functional connectomics and their test-retest reliabilities. We also aim to provide recommendations on use of these functional metrics for characterizing the brain connectome at a systems neuroscience level by summarizing the voxel-wise reliability maps of seven functional networks of a large-scale functional brain parcellation. Fig. 1 demonstrates a flowchart of the overall analytic strategies. Specifically, we first introduce the RFMRI measurements of human functional connectomes at the voxel level (Fig. 1A–D) and then briefly review various voxel-wise functional metrics (Fig. 1D), the test-retest reliabilities of which have been examined previously (Fig. 1E). Finally, these reliability maps are summarized into a large-scale functional parcellation of the human brain as defined in (Yeo et al., 2011) (Fig. 1F) by comparing the distribution of voxel-wise test-retest reliability values (Fig. 1G), the proportion of reliable voxels (Fig. 1H) and the ratio of reliable voxels (Fig. 1I) across the seven functional networks.

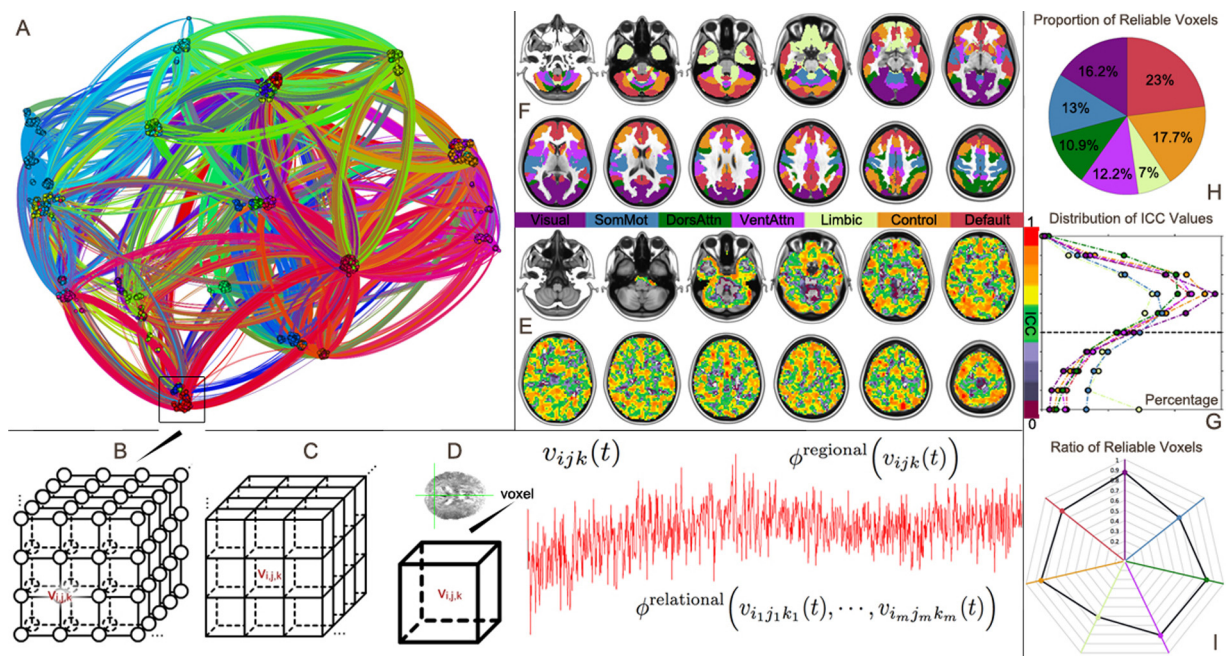


Fig. 1. A flowchart of the overall analytic strategies. A voxel-wise wiring graph adapted from Zuo et al. (2012) is depicted in (A). This brain graph comprises nodes and edges, part of which is enlarged in (B). The node is a 3D volumetric element (voxel v_{ijk} : i, j, k are the indices along the three dimensions in 3D space) as an unit of RFMRI data acquisition in millimeters (C). The temporal dynamics $v_{ijk}(t)$ of the human brain function can be measured for each voxel across the entire brain within seconds. For each voxel, various functional metrics can be calculated for characterizing both regional and relational metrics (D). We first reviewed various voxel-wise metrics, the test-retest reliabilities of which have been examined previously with mapping the intraclass correlation (ICC) voxel-wise (E). This figure is reproduced from Zuo et al. (2013). Next, these voxel-wise reliability maps were summarized into a large-scale functional brain parcellation including visual (Visual), somatomotor (SomMot), dorsal attention (DorsAttn), ventral attention (VentAttn), limbic (Limbic), frontoparietal (Control) and default (Default) networks (F). This figure is remade in terms of the human brain parcellation data from Yeo et al. (2011), Buckner et al. (2011), Choi et al. (2012). Finally, the distribution of voxel-wise ICC values (G: histogram graph), the proportion of reliable voxels (H: pie graph) and the ratio of reliable voxels (I: spider graph) are visualized across these seven large-scale prior functional networks.

2. Functional metrics of brain connectomes with RFMRI

The basal metabolism of the human brain measured during rest state (i.e., eyes closed, awake, and no specific cognitive task) represents 20% of the total body energy consumption, which highlights the importance of studying resting state brain function (Raichle, 2006; Raichle and Mintun, 2006). RFMRI was initially proposed to study low-frequency spontaneous neural activity in the motor system (Biswal et al., 1995). Since then, this technology has been widely used to study human brain function over the last two decades; after rapid development, it has become a powerful tool for functional connectomics (Biswal et al., 2010; Zuo et al., 2012; Smith et al., 2013a,b). As of February 16, 2014, a PubMed literature search (keywords: **resting AND brain AND fmri**) revealed that 4455 brain research articles using RFMRI have been published. As the first large-sample validation of RFMRI, in 2010, Dr. Biswal and 53 colleagues around the world published a milestone paper that highlighted a call for discovery science via sharing more than 1400 RFMRI datasets and demonstrated data-sharing advantages for the study of the human brain function. This work has greatly accelerated the study of human brain function and multidisciplinary cooperation (Biswal et al., 2010).

The human brain is a complex and dynamic system that contains massive processing units (neuron, circuit, column, area, etc.) at different scales (Lichtman and Denk, 2011), each of which has its own dynamics and are mutually wired into a functional connectome (Fig. 1A). Many theories have been proposed to model brain structure-to-function relationships or functional connectomics (Deco et al., 2013; Gerstner et al., 2012). The 'gold standard' of the functional connectomes would be the entire wiring diagram derived at the neuron level or mapping the activity of every neuron in the human brain as proposed by the Brain Research through Advancing Innovative Neurotechnologies (BRAIN) Initiative or the

Brain Activity Map Project (Alivisatos et al., 2012, 2013b; Zador et al., 2012; Kandel et al., 2013). From the perspective of experimental science, although some ideas have been proposed to achieve mapping the neuron-level functional connectomes (Alivisatos et al., 2013a), at the current stage, RFMRI still serves as a brain-mapping tool with the best trade-off between spatial and temporal resolutions to measure the outputs of this complex and dynamic system (i.e., RFMRI a voxel of millimeters in a time-window of seconds).

The complexity of the human brain functional connectomics is reflected in its massive amount of neurons and their hierarchical integration across multiple scales (Park and Friston, 2013). Brain mapping at the voxel level not only generates high-resolution (voxel-wise) basis maps of functional metrics for further investigation of the human brain at three large scales (i.e., local area, subnetwork, and the entire connectome) but also serves as a translational stage of developing optimal computation platform and efficient algorithms for neuron-wise functional connectomics regarding the complexity. This situation motivates the focus of the current review as voxel-wise metrics of the human functional connectomes with RFMRI. A voxel-wise wiring graph has been generated based upon 1003 RFMRI datasets (Zuo et al., 2012) and is illustrated in Fig. 1A, in which the functional signal $v_{ijk}(t)$ of a voxel v_{ijk} (i, j, k are the indices along the three dimensions in 3D space) was measured by RFMRI (Fig. 1B/C/D). There are two categories (Tononi et al., 1994; Friston, 2009, 2005) of RFMRI computational methods for the characterization of the functional architecture of the human brain with voxel-wise metrics: (1) the temporal dynamics of the single voxel $\phi(v_{ijk}(t))$ (i.e., functional specialization/segregation at the voxel level), and (2) the relationships among multiple voxels $\phi(v_{i_1j_1k_1}(t), \dots, \phi(v_{i_mj_mk_m}(t)), m \geq 2$ (i.e., functional integration at the voxel level)). In following sections, we will primarily review these voxel-wise metrics in the field of functional connectomics, the test-retest reliabilities of which have been investigated in the

literature. More comprehensive reviews (not limited to the voxel level) on functional connectomics methodology can be found in the literature (e.g., [Zhang and Raichle, 2010](#); [Wang et al., 2010](#); [Cole et al., 2010](#); [Margulies et al., 2010](#)).

2.1. The regional characteristics of a single voxel

In a seminal paper, [Biswal et al. \(1995\)](#) proposed the use of the root mean square (RMS) of the low-frequency fluctuations in the RFMRI time series to measure the intensities of the moment-to-moment fluctuations in a region and noted that gray matter signals have 60% higher RMS values than white matter. However, most researchers overlooked this metric when it was first presented. Dr. [Zang and his colleagues \(2007\)](#) extended the RMS metric to the frequency domain by using the fast Fourier transform and proposed a voxel-wise measure of the amplitude of low-frequency fluctuations (ALFF). This work represented a major contribution by mapping the voxel-wise spatial distribution or regional variation of ALFFs across the entire brain ([Zang et al., 2007](#)). To further enhance the ALFF contrasts between brain tissues (e.g., gray matter) and non-brain tissues (e.g., large vessels), the same team developed a normalized version of ALFF, namely, fractional ALFF (fALFF) ([Zou et al., 2008](#)). As demonstrated in Fig. 3 by [Zuo et al. \(2010a\)](#), ALFF was markedly greater than fALFF near large blood vessels, and in areas adjacent to cerebrospinal fluid (particularly in the brainstem), which are susceptible to the effects of pulsatile motion. In this regard, fALFF may preferably be used because it standardizes the power spectra and is robust against physiological noise. [Kannurpatti and Biswal \(2008\)](#) employed the standard deviation (SD) of the low-frequency (0.01–0.1 Hz) band-pass filtered RFMRI time series to measure the resting state fluctuation amplitude (RSFA). The theoretically strict equivalence between SD-based RSFA and ALFF was demonstrated mathematically in a short report (<http://hdl.handle.net/10101/npre.2010.4379.1>). In the field of neuroscience, above amplitude measurements have been increasingly recognized as biologically meaningful indices of the intra-individual moment-to-moment variability of human brain function ([Garrett et al., 2013, 2011](#)) and have demonstrated associations with task-induced brain activity and behavioral performance ([Mennes et al., 2011](#); [Zou et al., 2013](#)). In contrast to time-domain metrics such as RSFA, ALFF is calculated in the frequency domain and thus has advanced the simultaneous examination of human brain functional specialization across different frequencies. Similarly, [McAvoy et al. \(2008\)](#) introduced the use of power spectral densities to analyze all low-frequency points via repeated measure ANOVAs. Taking a step further, [Zuo et al. \(2010a\)](#) proposed ALFF metrics based on different frequency ranges defined in terms of the neuronal oscillation theory ([Buzsaki and Draguhn, 2004](#)). The authors revealed the specificity of the slow-4 (0.027–0.073 Hz) of the ALFF to the basal ganglia, which represented a prelude to the study of intra-individual variability in RFMRI signals across different frequencies. Notably, in computing the ALFF, a summary of the amplitudes within the low-frequency range can be achieved with two different norms: L^2 and L^1 , which are formulated below

$$\text{ALFF}^{L^2} = \sqrt{\sum_{k:f_k \in [0.01, 0.1]} \frac{a_k^2(f) + b_k^2(f)}{N}}, \quad (1)$$

$$\text{ALFF}^{L^1} = \sum_{k:f_k \in [0.01, 0.1]} \sqrt{\frac{a_k^2(f) + b_k^2(f)}{N}}. \quad (2)$$

In theory, there are no intrinsic differences in the overall spatial patterns and regional variations between the two ALFF metrics, although the absolute value of the L^1 -based ALFF is always greater

than that of the L^2 -based ALFF. Although the test-retest reliabilities have not been examined, many other voxel-wise metrics of the single voxel activity including the degree of power-law fitting ([Kiviniemi et al., 2000](#)), the fractal dimension or Hurst exponent ([Maxim et al., 2005](#); [Wink et al., 2008](#)), the multi-scale or approximate entropy ([Smith et al., 2014](#); [Liu et al., 2013a](#)) and the Lyapunov exponent ([Xie et al., 2008](#)) have also been proposed to characterize various nonlinear features and the complexity of RFMRI signals.

2.2. The relational characteristics among multiple voxels

The relationships among multiple RFMRI time series can be categorized into functional and effective connectivity ([Friston, 1994](#); [Park and Friston, 2013](#)). Functional connectivity characterizes the statistical dependence among RFMRI time series across time without any consideration for causality, and effective connectivity describes causality ([Friston, 2011](#)). Currently, although causal analyses of RFMRI time series remain controversial ([Smith et al., 2011](#)), the exploration of such methodology ([Friston et al., 2011](#)) and its applications ([Morgan et al., 2011](#)) to both healthy and clinical populations may offer insight into our understanding of the complexity of human brain function regarding the extreme complexity of hemodynamic responses and their regional variations. Thus, here, we do not focus on metrics that measure effective connectivity, for example, dynamic causal modeling (DCM) or granger causality (GC), and we recommend certain published reviews to the interested readers ([Hu et al., 2011](#); [Stephan and Friston, 2010](#)). Various functional connectivity metrics will be surveyed below.

[Biswal et al. \(1995\)](#) used the Pearson's correlation coefficient of RFMRI time series between two voxels to measure the functional connectivity between that pair of voxels and introduced the intrinsic functional connectivity (iFC) approach ([Kelly et al., 2012](#)). The correlation coefficient has now been expanded to a variety of more meticulous metrics for characterizing iFC at the scales of local regions, functional subsystems and the entire connectome. For a given local region, the mean of the correlation coefficients of spontaneous low-frequency (COSLOF) components between possible pairs of voxel time series in the region has been proposed to quantify the overall iFC of this region ([Li et al., 2002](#)). The same method has also been used to study iFC within a functional subsystem; i.e., network homogeneity ([Uddin et al., 2008](#)). These methods can be easily generalized into voxel-wise metrics to measure local functional homogeneity (e.g., [Deshpande et al., 2009](#); [Tomasi and Volkow, 2010](#); [Zuo et al., 2013](#)). The most common method to study the functional network iFC is the seed-based approach; this approach first chooses a region of interest (the seed region) and then calculates the correlation coefficients of the RFMRI time series of any other voxel with the seed voxel, which results in a seed-specific functional network iFC map ([Biswal et al., 1995](#); [Fox et al., 2005](#)). This idea of using a region of interest can be extended to a set of regions with a common anatomical constraint. The iFC between inter-hemispheric regions or voxels (i.e., functional homotopy) has been systematically investigated at the level of both large-scale parcellations ([Stark et al., 2008](#)) and individual voxels ([Zuo et al., 2010c](#); [Anderson et al., 2011a](#)); this approach has specifically been used for mapping voxel-mirrored homotopic connectivity (VMHC), which has been proposed for the trajectory delineation of high-resolution functional homotopy across the human lifespan ([Zuo et al., 2010c](#)). Finally, several methods based on the covariance or correlation matrix derived from RFMRI time series that are not dependent on a specific area can produce multiple functional networks simultaneously; these methods include component analysis (e.g., [Beckmann et al., 2005](#); [Kiviniemi et al., 2003](#); [Zhong et al., 2009](#)) and data clustering (e.g., [Bellec et al., 2010](#); [Cordes et al., 2002](#); [van den Heuvel et al., 2008](#)). One particular challenge, the correspondence between a set of group-level components

and those at the individual level, has initially been addressed for group-level independent component analysis (ICA) with spatial-temporal dual regression (drlICA) (Filippini et al., 2009; Zuo et al., 2010b; Erhardt et al., 2011) and individual network mining algorithms based upon intra- and inter-individual reproducibility of components (e.g., Yang et al., 2008, 2012; Pendse et al., 2011).

The correlation coefficient has also been used to construct a functional connectivity pattern of all of the brain's functional networks (i.e., functional connectomes), which can be converted into a graph and quantified by various metrics using graph theory to bridge the structure-function relationships of the human brain (Sporns et al., 2000; Rubinov and Sporns, 2010). Many graphical attributes of the large-scale functional connectomes such as small-world, degree distribution, key/hub node, network efficiency, modularity, cost and rich club have been systematically investigated (Wang et al., 2010; He et al., 2009; Bullmore and Sporns, 2009, 2012). Most previous studies using graph theory have emphasized network features (e.g., regions that are highly connected or hub regions) at large scales (typically 50–1000 brain regions). The nature of these nodal metrics as measures of the strengths of functional connectivities has been overlooked. Dr. Buckner was the first to consider the nodal degree centrality (DC) at the voxel level as a measure of functional connectivity and to relate it to the brain energy cost (Buckner et al., 2009), which has been replicated recently (Liang et al., 2013; Tomasi et al., 2013). To characterize multi-scale topological properties of network nodes and connections, this DC metric has recently been generalized to various voxel-wise network centrality metrics (VNCM) including subgraph centrality (SC), eigenvector centrality (EC) and pagerank centrality (PC) and employed to reveal the multi-scale nature of human functional connectomes at the voxel level (Zuo et al., 2012). Any of these centrality metrics only reflects part of the functional connectome's properties, thus highlighting the need for developing and combining multiple metrics to characterize functional brain organization. Of note, common centrality metrics (e.g., DC and EC) have been recognized as influenced by different sizes of network communities in the field of food sciences (Jordan et al., 2006), although researchers in brain connectomics just noticed this effect recently (Power et al., 2013b). In network sciences, some novel measures of centrality exist for characterizing the network nodal importance without the bias of community size (e.g., Qi et al., 2012, Laplacian centrality) and (e.g., Zuo et al., 2012, subgraph centrality with certain first largest eigenvalues), which should be considered in future studies on brain connectomics.

As a connectivity measure, the correlation coefficient is simple and easy to implement, and it has been validated, in most cases, as effectively characterizing iFC (Hlinka et al., 2011). However, the use of the correlation coefficient in the study of resting-state functional brain activity has theoretical limitations because the observed RFMRI time series are noisy and intrinsically auto-correlated in the time domain, which violates the requirement for independent, normally distributed samples for the accurate estimation of Pearson correlation coefficients. Certain distribution-free, non-parametric correlation metrics can remedy this disadvantage of the Pearson's correlation coefficient. The rank-based Kendall's coefficient of concordance (KCC) has been proposed to measure the regional homogeneity (ReHo) of spontaneous neural activities (Zang et al., 2004) and can be viewed as a non-parametric voxel-wise version of COSLOF (Zuo et al., 2013), although the spatial extents of the two methods were distinct in the original literature (Li et al., 2002; Zang et al., 2004).

$$KCC = 12 \frac{\sum_{i=1}^n (\bar{R}_i)^2}{n^3 - n} - 3 \frac{n+1}{n-1}. \quad (3)$$

Eq. (3) formulates the computation of ReHo (n is the number of time points in the RFMRI time series) and clearly indicates ReHo's advantages in theory; i.e., this metric integrates noise-filtering operations in both the time domain (the order-rank filter) and the spatial domain (the mean-rank filter). Thus, this metric has high robustness against tempo-spatial noise and outliers, which makes it an RFMRI metric with high test-retest reliability (Zuo et al., 2013). This adaptive tempo-spatial noise suppression as the data-driven nature of ReHo is very attractive in processing RFMRI data under complex experimental conditions (e.g., Dong et al., 2014). Researchers have demonstrated the utility of ReHo to link individual differences in local functional homogeneity quantified with ReHo to cognitive performance (Tian et al., 2012; Wang et al., 2014). Beyond the high test-retest reliability, two recent studies related the local functional homogeneity to complexity of information processing across spatial and temporal domains, respectively (Jiang et al., 2014; Anderson et al., 2014), suggesting the neurobiological meanings of local functional homogeneity. Of note, there is another ReHo-like voxel-wise functional metric, namely, local functional connectivity density (IFCD), which attempts to address the tempo-spatial noise issue with an explicit threshold of the signal-to-noise ratio (SNR) and spatial smoothing (Tomasi and Volkow, 2010); however, it is not as adaptive as ReHo.

The local functional homogeneity varies remarkably across the whole brain at voxel level (Zuo et al., 2013). This finding invokes the voxel-wise graphs or connectomes. Currently, with full adjacency matrices available for brain connectomics at the voxel level, we are entering into an arena of developing various voxel-wise metrics by harnessing classic matrix-based graph theory (e.g., Zuo et al., 2012; Estrada and Higham, 2010, subgraph centrality), recent advances in massive graph analysis and the increased ability of the high-performance computing (e.g., Wang et al., 2013) for discovery sciences of the human brain function in an unbiased way (Turk-Browne, 2013). These full brain voxel-wise graphs and their dynamics (Allen et al., 2014) will lead to big data for neuroscience.

2.3. Computational platforms and big data sharing

Software plays an important role in discovering the human brain functional connectomics at the voxel level. A growing number of software packages are being developed to compute the voxel-wise metrics reviewed above. The Resting-State fMRI Data Analysis Toolkit (REST) (Song et al., 2011) is widely used to estimate these metrics in various applications because of its easy-to-use graphical user interface (GUI). This toolkit also has an advance plugin to facilitate batch processing; i.e., the Data Processing Assistant for Resting-State fMRI (DPARSF) (Yan and Zang, 2010). Graph theory-based network metrics can be computed using the brain connectivity toolbox (BCT: <http://www.brain-connectivity-toolbox.net>) (Rubinov and Sporns, 2010). The graph theory toolkit for network analysis (GRETNA: <http://www.nitrc.org/projects/gretna>) has also been developed for brain connectomics and is similar to the BCT but has a friendly GUI. Notably, REST, BCT and GRETNA were all built within the MATLAB programming environment, and thus are not completely open-source toolboxes. There are some other packages that are based on MATLAB that can be found at the RFMRI network website (RFMRI.org), which was initially developed by Dr. Chao-Gan Yan and aims to share ideas, comments, resources, tools, experiences and data with researchers from the community of RFMRI brain connectomes.

Beyond the RFMRI methods and various software, a large-sample publicly available RFMRI data pool is essential for multidisciplinary researchers to accelerate the development of new methodology and to evaluate the existing methods and toolboxes. Before 2010, most neuroimaging studies were performed

with sample sizes of approximately 10–100, which clearly limit the statistical power of functional connectomics in studying brain development, behavioral association and disorders. The sample sizes obtainable from a single imaging site are obviously constrained by scanning costs and funding support. At the end of 2008, Drs. Bharat Biswal and Michael Milham contacted researchers in the RFMRI community to share their data. At that point in time, Professor Yu-Feng Zang of Beijing Normal University was the first to give his full support for this grassroots data-sharing idea by generously depositing a total of 198 RFMRI datasets. Subsequently, the ‘1000 Functional Connectomes Project’ (FCP: http://fcon_1000.projects.nitrc.org) (Biswal et al., 2010) was launched and now shares nearly 1500 RFMRI datasets for human brain function discovery sciences. Dr. Milham further developed FCP into the International Neuroimaging Data-sharing Initiative (INDI: http://fcon_1000.projects.nitrc.org/indi) to openly share neuroimaging data for science (Milham, 2012). Within the INDI, the ADHD200 (http://fcon_1000.projects.nitrc.org/indi/adhd200) (Fair et al., 2012) and ABIDE (http://fcon_1000.projects.nitrc.org/indi/abide) (Di Martino et al., 2014) provide the rich resources of multimodal neuroimaging datasets for brain development and disorders, accelerating the pace of discovery sciences related to these two mental disorders. Currently, many studies have been performed based on these public datasets, showing the advantages of sharing big data with the community (Mennes et al., 2013).

Researchers have increasingly recognized that the challenges of human brain connectomics would require the establishment of an integrated computational platform to mine the extensive data of the human brain (Akil et al., 2011). Although still in its infancy stage, neuroinformatics has been proposed to achieve this system via development of computation-integrated databases. As the pipeline of the FCP, the FCP_1000 scripts naturally combine and integrate various commands from open-source neuroimaging toolboxes, such as AFNI (Cox, 2012) and FSL (Jenkinson et al., 2012), for the large-scale data analysis in FCP. Regarding the advances in data processing and standardization, the FCP pipeline has been further extended into two pipelines: the Configurable Pipeline for the Analysis of Connectomes (C-PAC: <http://fcp-indi.github.io>) and the Connectome Computation System (CCS: <http://lfcd.psych.ac.cn/ccs.html>). Specifically, the C-PAC is an open-source software pipeline for automated preprocessing and analysis of RFMRI datasets. This pipeline has been specifically optimized for large datasets and validated in a recent work (Di Martino et al., 2014). From a different aspect of development, the CCS extends the functions of FCP scripts onto the cortical surface by integrating FreeSurfer (Fischl, 2012) and Caret (Van Essen, 2012) commands, aiming to provide a computational platform for multimodal neuroimaging brain connectomics. The CCS contains several unique modules including quality control procedure (QCP), brain connectome visualization (BCV), test-retest reliability (TRT), multimodal brain parcellation (MBP), and connectome-wide association (CWA). This pipeline has been employed to study local functional homogeneity (Zuo et al., 2013; Jiang et al., 2014), morphological correlates of individual differences in fearful face recognition (Zhao et al., 2013) and Chinese Tai Chi Chuan performance (Wei et al., 2013, 2014), lifespan changes of the functional connectomes (Cao et al., 2014; Yang et al., 2014), and default network connectivity in obsessive-compulsive disorder (Peng et al., 2014). Both C-PAC and CCS can be easily integrated into a neuroimaging database.

The Human Connectome Project (HCP: <http://www.humanconnectome.org>) released a promising data-computation integrated informatics platform to share and mine the big data generated from 1200 healthy adults. This system is designed with the eXtensible Neuroimaging Archive Toolkit (XNAT) (Marcus et al., 2007) including two interoperable components: ConnectomeDB

and Connectome Workbench (Marcus et al., 2011, 2013). The ConnectomeDB is a data management system to house all image data, clinical evaluations, behavioral data and more, and ideally should work seamlessly with Connectome Workbench, an interactive, multidimensional visualization system. In the future, an efficient, reliable and powerful platform should be designed for high-throughput neuroimaging analysis by integrating various pipelines, databases and high performance computing infrastructures (e.g., Lavoie-Courchesne et al., 2012).

3. Test-retest reliability in functional connectomics

We have briefly reviewed the high-resolution (i.e., voxel-wise) metrics of the human brain function. As mentioned, our aim with this review is to provide a systematic overview on the test-retest reliability of these voxel-wise functional metrics and further a reference on uses of these metrics to study the human functional connectome markers in brain disorders (Singh and Rose, 2009). In this section, the test-retest reliability of common functional metrics will be summarized at the level of system neurosciences by integrating previously published papers on reliabilities (Shehzad et al., 2009; Zuo et al., 2010a,b,c, 2012, 2013) with a large-scale functional parcellation of the human brain (Yeo et al., 2011).

3.1. The concept of test-retest reliability

Test-retest reliability is an important concept in social, behavioral, physical, biological and medical sciences. It is crucial for building and choosing reliable measures because various factors interfere with the actual measurement procedure (Nakagawa and Schielzeth, 2010). From a statistical perspective, test-retest reliability is a group-level statistic and refers to the temporal or intra-individual stability of an index measured across multiple occasions in a group of subjects. Using blood pressure in medicine as an example, test-retest reliability refers to the intra-individual or within-subject (i.e., measurements of blood pressure from the same person at two or more time points) variability relative to the inter-individual or between-subject (i.e., different measurements of blood pressure from a group of persons) variability.

In functional connectomics, given a functional metric ϕ at a voxel v , the intra-class correlation (ICC) is commonly used to quantify its test-retest reliability (Shrout and Fleiss, 1979). Linear mixed models (LMMs) can model both intra- and inter-individual variability (Zuo et al., 2013; Chen et al., 2013; Bernal-Rusiel et al., 2012, 2013). To calculate the ICC for voxel v , we considered a random sample of n subjects with d repeated measurements of a continuous variable ϕ . ϕ_{ij} (for $i = 1, \dots, d$ and $j = 1, \dots, n$) denotes the voxel-wise metric from the j th participant's i th measurement occasions. We applied a two-level LMM to decompose ϕ_{ij} at each voxel as the following:

$$\phi_{ij} = \lambda_{0j} + e_{ij}, \quad \lambda_{0j} = \mu_{00} + p_{0j}, \quad (4)$$

where μ_{00} is a fixed parameter (the group mean) and p_{0j} and e_{ij} are independent random effects normally distributed with a mean of 0 and variances σ_p^2 and σ_e^2 . The term p_{0j} is the participant effect, and e_{ij} is the measurement error. The voxel-wise whole brain statistical map can be built at the group level by estimating the statistics of testing if the μ_{00} in the model (4) with all test-retest scans from all participants significantly differs from 0. The voxel-wise ICC map of ϕ is also computed by estimating the test-retest reliability defined as

$$ICC(\phi) = \frac{MS_b(\phi) - MS_w(\phi)}{MS_b(\phi) + (d - 1)MS_w(\phi)} = \frac{\sigma_p^2}{\sigma_p^2 + \sigma_e^2}. \quad (5)$$

Here, MS_w is the statistical variance of the difference in ϕ between all time points (i.e., within-subjects mean squared error), whereas MS_b represents the variance between all possible subject pairs (i.e., between-subjects mean squared error). A detailed version of Eq. (5) is available in Appendix of (Zuo et al., 2010b). To avoid negative ICC values and obtain more accurate estimation of the sample ICC, the variance components in Model (4) are usually estimated with the restricted maximum likelihood (ReML) approach with the covariance structure of an unrestricted symmetrical matrix (Zuo et al., 2013).

3.2. The need for biomarkers and correction for attenuation

Eq. (5) indicates that high test-retest reliabilities require the following: (1) a small variability within subjects to ensure the temporal stability of the measures of a metric and (2) a large variability between subjects that allows for the distinguishing of different individuals. The two features ensure that the high test-retest reliability is one of necessary requirements for developing a biomarker. The application of functional connectomics as a longitudinal biomarker requires reliability, sensitivity and specificity to longitudinal changes such as in mapping growth charts of the human brain function and its relationship with various neurocognitive performance (Dosenbach et al., 2010; Erus et al., 2014; Satterthwaite et al., 2014; Gur et al., 2014). The ideal measures should be not only proven stable over time in the absence of disease but also highly attuned to longitudinal decline or improvement. Ultimately, the best measures will allow detection of meaningful clinical benefits over short intervals in a few subjects as well as have high information content relative to individual disease processes. This goal may require trade-offs among reliability and sensitivity or validity as well as specificity of a functional connectome metric.

Various sources of noise are unavoidably included in the measurement of every variable, making reliable and accurate estimation of relationships between the variables challenging. Previous studies on RFMRI or functional connectomes have shown that there are many confounding variables, such as machine noise, scanner type, body heat, cardiac and respiration artifacts, head motion, experimental instructions, data pre-/post-processing strategies, and data standardization (Yan et al., 2013b). In many cases, researchers aim to investigate the associations between brain and disease (Rubinov and Bullmore, 2013; Jiang et al., 2013; Jiang, 2013) or brain and behavior or other types of brain associations (Milham, 2012) by estimating correlations between two variables (at least one of which is a functional measure of brain activity). In practice, we can measure two variables x_0^1 and x_0^2 with outcomes $x^1 = x_0^1 + n^1$ and $x^2 = x_0^2 + n^2$ that are polluted by noises n^1 and n^2 . In statistics, the correction procedure for attenuation from classical test theory indicates how the reliabilities of the measurements affect the correlation between the two variables (Muchinsky, 1996; Carmines and Zeller, 1979), as formulated below

$$\text{CoRR}(x^1, x^2) = \text{CoRR}(x_0^1, x_0^2) \sqrt{\text{ICC}(x^1)\text{ICC}(x^2)}. \quad (6)$$

This equation highlights the role of the reliability of a measure as the upper bound of correlations involving that measure; i.e., the correlation between a pair of measures should never be higher than the reliability of either of the two measures. Therefore, beyond developing a biomarker, comprehensive estimations of the test-retest reliabilities of the metrics used in functional connectomics would be extremely valuable for providing a reference regarding how strongly the variables or measured properties affect the observed results and would thus guide explanations of the observed findings of both normal and abnormal brains.

3.3. Test-retest reliability of functional connectome metrics

Test-retest reliability was overlooked in RFMRI functional connectomes before the first test-retest reliability study of seed-based iFC was conducted (Shehzad et al., 2009). In that study, the authors reported high intra- and inter-session test-retest reliabilities of iFCs with several seeds within the DMN. Zuo and colleagues systematically mapped out the voxel-wise test-retest reliabilities of the ALFF, fALFF, drICA, VMHC, VNCM, and ReHo (Zuo et al., 2010a,b,c, 2012, 2013). These work employed the 75 NYU test-retest datasets (three RFMRI scans of each individual and a total of 25 healthy adults) (www.nitrc.org/projects/nyu_trt) to compute the intra-session ($d=2$) and inter-session ($d=2$) ICC for those voxel-wise functional metrics. The intra-session ICC was estimated based on Scans 2 and 3, which were 45 min apart and conducted in a single scan session (i.e., short-term retest). The inter-session ICC was computed by using individual metrics from Scan 1 and individual mean metrics from Scans 2 and 3, which occurred 5–16 months after Scan 1. The ICC values are categorized into five common intervals (Landis and Koch, 1977): $0 < \text{ICC} \leq 0.2$ (slight); $0.2 < \text{ICC} \leq 0.4$ (fair); $0.4 < \text{ICC} \leq 0.6$ (moderate); $0.6 < \text{ICC} \leq 0.8$ (substantial); and $0.8 < \text{ICC} < 1.0$ (almost perfect). A metric with moderate to almost perfect test-retest reliability ($\text{ICC} \geq 0.4$) is commonly expected in practice.

To summarize the common findings of these test-retest studies, we conducted a meta-summary reliability analysis (MSRA) at the systems neuroscience level by integrating voxel-wise ICC maps of these functional metrics into a comprehensive functional brain parcellation. This parcellation was derived in a previous study (Yeo et al., 2011) based on RFMRI datasets from 1000 healthy people acquired with a single scanner. The study first divided the cortex into seven large-scale functional networks that include the visual (Visual), somatomotor (SomMot), dorsal attention (DorsAttn), ventral attention (VentAttn), frontoparietal or control (Control), limbic (Limbic) and default (Default) networks (Fig. 1F). The seven networks were further mapped onto the cerebellum and the striatum (Buckner et al., 2011; Choi et al., 2012). The methodological details of MSRA are described below.

MSRA aims to answer two questions: (Q1) Which network had the greatest test-retest reliability? (Q2) Which measure had the greatest test-retest reliability? Accordingly, given a voxel-wise ICC map of one functional metric $\text{ICC}(\phi(v))_{v=1,\dots,N}$ where N is the number of voxels, we calculated the following three quantities to compare the test-retest reliability of this metric across the seven large-scale functional networks $K_i(v)_{v=1,\dots,N_i}$, where $N_{i=1,\dots,7}$ is the number of voxels within the i th functional network:

- **Distribution of ICC values** (Fig. 1G) is measured with the histogram of the voxel-wise ICC values in a functional network K_i , i.e.,

$$h(K_i) = \left\{ \# v \in K_i \mid (j-1) \times 0.1 \leq \text{ICC}(\phi(v)) \leq j \times 0.1, j = 1, \dots, 10 \right\}.$$

- Proportion of reliable voxels (Fig. 1H) is defined as the percentage of whole brain voxels showing moderate to almost perfect test-retest reliability within a functional network K_i , i.e.,

$$p(K_i) = \frac{\#\{v \in K_i \mid \text{ICC}(\phi(v)) \geq 0.4\}}{\#\{v \mid \text{ICC}(\phi(v)) \geq 0.4\}}.$$

- Ratio of reliable voxels (Fig. 1I) is the percentage of reliable voxels within a specific functional network K_i , i.e.,

$$r(K_i) = \frac{\#\{v \in K_i | \text{ICC}(\phi(v)) \geq 0.4\}}{\#\{v \in K_i\}}.$$

To answer the above two questions, we calculated the three quantities for each of these eight voxel-wise functional metrics (i.e., PCC-iFC, ALFF, fALFF, drlICA, VMHC, DC, EC, ReHo) by using their test-retest reliability maps (e.g., Fig. 1E) across the seven large-scale functional networks in MNI152 2-mm standard space (Fig. 1F): Visual (21,740 voxels); SomMot (22,180 voxels); DorsAttn (15,421 voxels); VentAttn (17,743 voxels); Limbic (13,589 voxels); Control (24,488 voxels); and Default (34,000 voxels). Of note, to create a unified ICC map of the test-retest reliabilities of the drlICA, we assigned the maximal ICC from among the 20 ICC maps of each voxel to that voxel. This may unfairly inflate the estimation of the three quantities. In future, a completely new analysis by using dual regression based upon the seven network confidence maps can address this issue (Zuo et al., 2010b; Yeo et al., 2011). Similarly, using the PCC as a seed may bias the ICC of iFC. The effects of seed selection on ICC estimation need further investigation. These should be regarded as two limitations of the current MSRA method.

Beyond these three descriptive statistics, we also conducted a series of two-sample Kolmogorov-Smirnov (KS) tests (Marsaglia et al., 2003) to test whether the distributions of ICC values are significantly different between two networks or functional metrics. Specifically, given one of the eight functional metrics ϕ_i ($i = 1, \dots, 8$), we performed a two-sample KS test on the ICC values (Fisher-z transformed) of reliable voxels ($\text{ICC} \geq 0.4$) between each pair of the seven large-scale functional networks, resulting in a pair-wise KS significance matrix $\mathbb{A}(\phi_i)$. Similarly, given each of the seven functional networks K_i ($i = 1, \dots, 7$), we performed a two-sample KS test on the ICC values (Fisher-z transformed) of reliable voxels ($\text{ICC} \geq 0.4$) in this network between each pair of the eight functional metrics, leading to a pair-wise KS significance matrix $\mathbb{B}(K_i)$. Any KS test on ICCs between network or metrics was deemed significant if its p -value was less than $p_0 = 0.05 / ((6 \times 7 \times 8 + 7 \times 8 \times 7))$, which accounted for the Bonferroni-based correction for multiple comparisons. These matrices thus can be written as following formula,

$$\begin{aligned} \mathbb{A}(\phi_i)_{i=1,\dots,8} \\ = (a_{mn})_{m=1,\dots,7;n=1,\dots,7} \\ = \begin{cases} 1 & \text{if } p(\text{KS}(z(\text{ICC}(\phi_i) \geq 0.4)_{K_m}, z(\text{ICC}(\phi_i) \geq 0.4)_{K_n})) \leq p_0 \\ 0 & \text{if } p(\text{KS}(z(\text{ICC}(\phi_i) \geq 0.4)_{K_m}, z(\text{ICC}(\phi_i) \geq 0.4)_{K_n})) > p_0 \end{cases} \end{aligned}$$

and

$$\begin{aligned} \mathbb{B}(K_i)_{i=1,\dots,7} \\ = (b_{mn})_{m=1,\dots,8;n=1,\dots,8} \\ = \begin{cases} 1 & \text{if } p(\text{KS}(z(\text{ICC}(\phi_m) \geq 0.4)_{K_i}, z(\text{ICC}(\phi_n) \geq 0.4)_{K_i})) \leq p_0 \\ 0 & \text{if } p(\text{KS}(z(\text{ICC}(\phi_m) \geq 0.4)_{K_i}, z(\text{ICC}(\phi_n) \geq 0.4)_{K_i})) > p_0 \end{cases} \end{aligned}$$

The overlapping matrices of the significances of comparisons across the eight metrics $\mathbb{A} = \sum_{1 \leq i \leq 8} \mathbb{A}(\phi_i)$ or seven networks $\mathbb{B} = \sum_{1 \leq i \leq 7} \mathbb{B}(K_i)$ were used to determine which network or metric is most reliable. We performed all analyses equally to both intra-session (short-term: ~45 min) and inter-session (long-term: ~6 months) test-retest reliability. The findings of the intra-session reliability analysis were highly similar to those of the inter-session

reliability, but with substantially higher ICC values. We thus only present the main findings based upon the inter-session test-retest evaluation.

Fig. 2 depicts histograms of long-term ICC values within each of the seven large-scale functional networks across the eight functional connectome metrics. These curves revealed that the reliable voxels remain the smallest proportion in the limbic network across all the functional metrics except for ALFF. This finding most likely reflects the poor quality of RFMRI signals or signal loss within one dominant region of this network (i.e., the orbital frontal cortex). For most of these functional metrics, the high-order associative networks (Default, Control, DorsAttn and VentAttn) exhibited a larger percentage of reliable voxels wherein, especially for those voxels showing substantial to almost perfect reliability ($\text{ICC} \geq 0.6$) in contrast to the low-order primary networks (Visual, SomMot) containing a relatively lower percentage of reliable voxels across these functional metrics. This may be an indication of the rich variability of individual functional architecture within the high-level associative areas (Mueller et al., 2013). Regarding the reliability of different functional metrics, drlICA represented a metric of showing the largest percentage of reliable voxels within the seven networks, and ReHo was with the second largest percentage. The other remaining six metrics appeared to have no large differences in the proportion of reliable voxels, although fALFF and EC had the lowest proportions.

To assess differences in the proportion of reliable voxels in the full brain contributed by different functional networks, the quantity proportion of reliable voxels ($\text{ICC} \geq 0.4$) was visualized as pie graphs for all eight functional metrics (Fig. 3). These four high-order associative networks contributed more than 60% of the reliable voxels across the whole brain. Both the default and the control network were the two most important contributors to the whole brain reliability. This fact may not be surprising, considering that they are the two largest networks of the seven. To reduce the network-size effect, we further visualized the ratios of reliable ICCs for each of the seven networks for each of the eight metrics as spider graphs in Fig. 4. Again, this visualization confirmed the observation that the high-order associative networks contained a larger ratio of reliable voxels than the primary networks. Both default and control networks were still the two important players in this regard. drlICA, ReHo and VMHC were the three most reliable functional metrics regarding their spatial extents (i.e., the ratio of reliable voxels) across these seven large-scale networks.

Direct comparisons with the KS tests on the ICC values of all reliable voxels (≥ 0.4) across the seven functional networks as well as across the eight functional metrics validated our these findings statistically (Fig. 5). Specifically, the overlapping matrix \mathbb{A} revealed that the limbic networks demonstrated significant differences in long-term ICC compared with the other four associative networks; importantly, these differences were consistent across all eight functional metrics. Without considering the limbic network, these association networks demonstrated more variable inter-network differences in long-term ICC values across all the functional metrics than the primary networks, echoing the previous observation in Fig. 4. The overlapping matrix \mathbb{B} indicated that drlICA, ReHo, VMHC and ALFF exhibited significant inter-metric differences in long-term ICC values across almost the seven networks, statistically confirming the observation in Fig. 4.

In this section, we focused only on the test-retest reliabilities of the above eight voxel-wise metrics in functional connectomics using the meta-summary analysis proposed. There are also several studies on the test-retest reliabilities of large-scale parcellation-based graph metrics (e.g., Wang et al., 2010; Braun et al., 2012). Generally, these studies have reported only moderate test-retest reliabilities (average ICCs < 0.5) of graph theory metrics, although these reliabilities can be improved to approximately 0.6 through

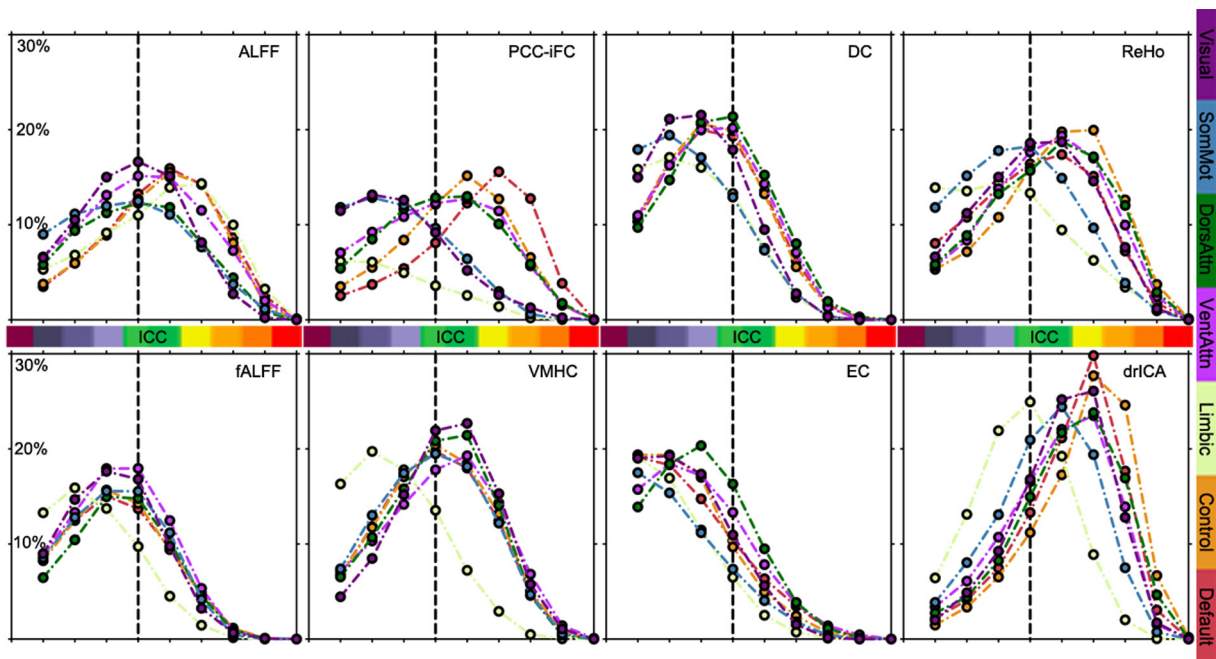


Fig. 2. The distribution of voxel-wise inter-session ICC across functional brain networks. Long-term (~6 months) test-retest reliabilities are measured with intra-class correlation (ICC) for the following eight functional metrics: amplitude of low-frequency fluctuations (ALFF); fractional ALFF (fALFF); intrinsic functional connectivity seeded by posterior cingulate cortex (PCC-iFC); voxel-mirrored homotopic connectivity (VMHC); degree centrality (DC); eigenvector centrality (EC); regional homogeneity (ReHo); and independent component analysis with dual regression (drICA). Given a functional metric, the histograms of its voxel-wise ICC values within each of the prior seven functional networks defined as in Fig. 1 are plotted with 10 bins of the ICC range from 0 to 1 (the first bin 0–0.1 data are not shown). The dash lines indicate the critical ICC for reliable voxels (i.e., $\text{ICC} \geq 0.4$).

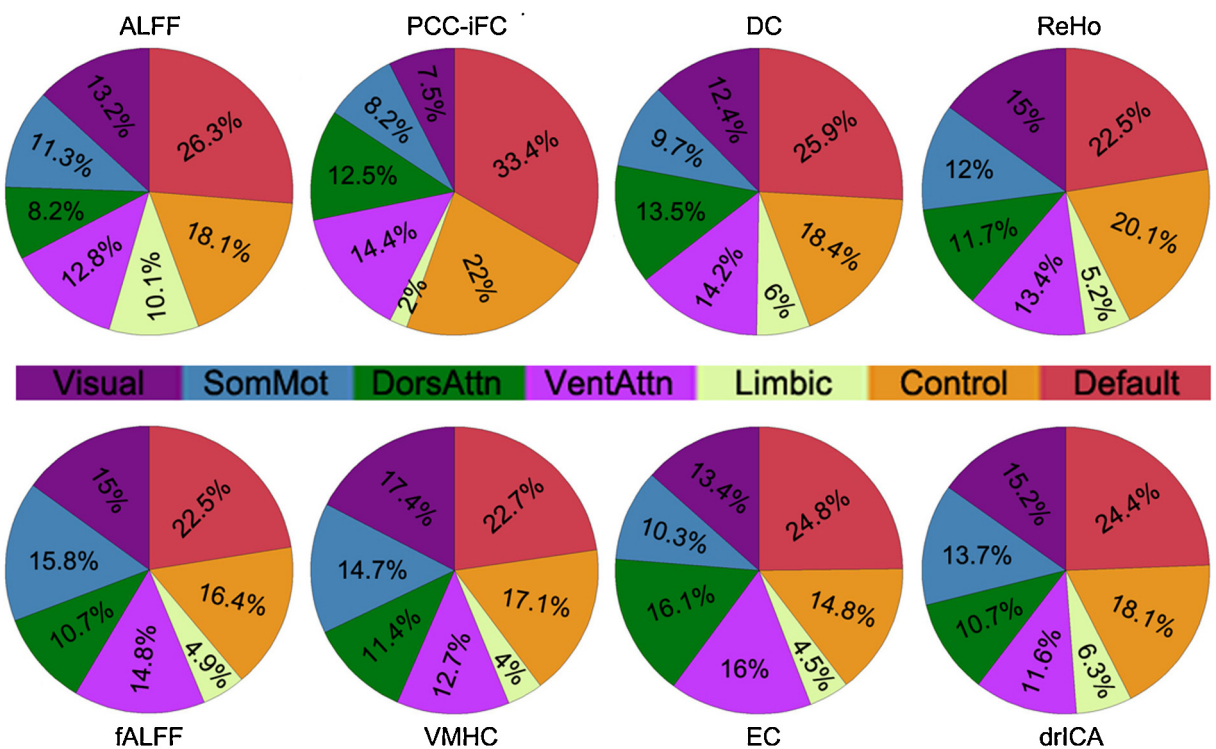


Fig. 3. The proportion of reliable voxels across functional brain networks. Long-term (~6 months) test-retest reliabilities were measured with intra-class correlation (ICC) for the following eight functional metrics: amplitude of low-frequency fluctuations (ALFF); fractional ALFF (fALFF); intrinsic functional connectivity seeded by posterior cingulate cortex (PCC-iFC); voxel-mirrored homotopic connectivity (VMHC); degree centrality (DC); eigenvector centrality (EC); regional homogeneity (ReHo); and independent component analysis with dual regression (drICA). Given a functional metric, the percentages of whole brain voxels showing moderate to almost perfect test-retest reliability ($\text{ICC} \geq 0.4$) within each of the prior seven functional networks defined as in Fig. 1 are depicted as pie graphs.

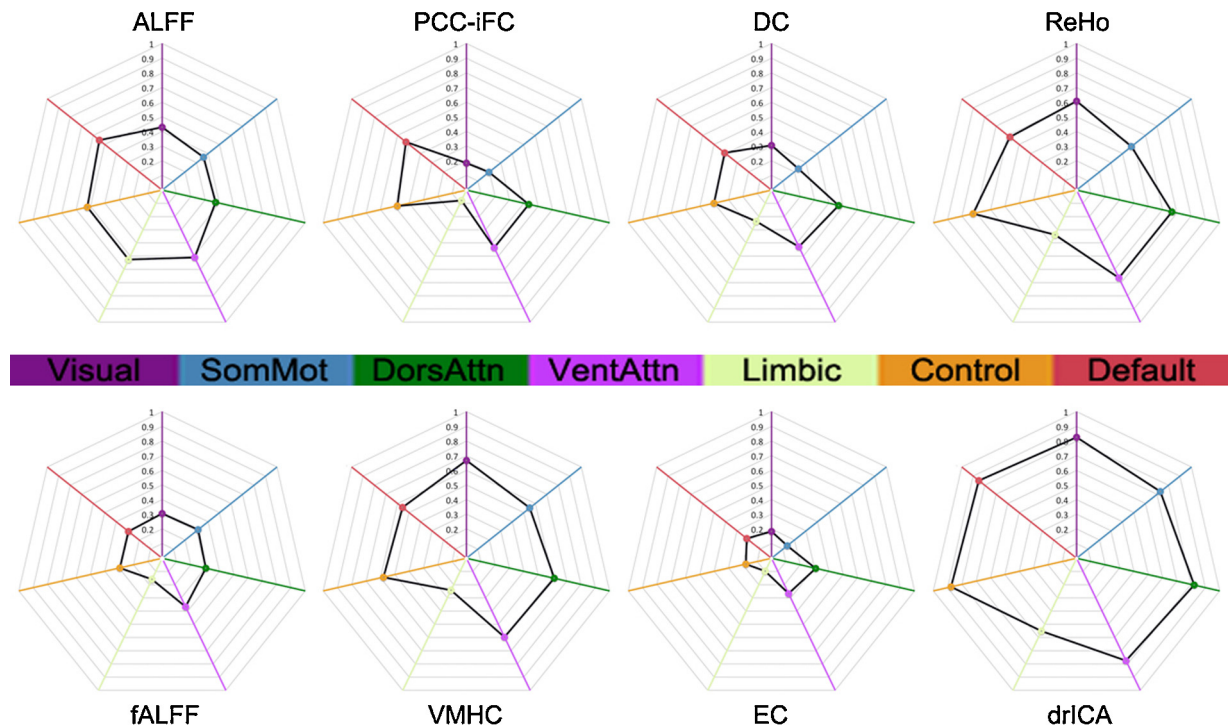


Fig. 4. The ratio of reliable voxels across functional brain networks. Long-term (~6 months) test-retest reliabilities were measured with intra-class correlation (ICC) for the following eight functional metrics: amplitude of low-frequency fluctuations (ALFF); fractional ALFF (fALFF); intrinsic functional connectivity seeded by posterior cingulate cortex (PCC-iFC); voxel-mirrored homotopic connectivity (VMHC); degree centrality (DC); eigenvector centrality (EC); regional homogeneity (ReHo); and independent component analysis with dual regression (drICA). Given a functional metric, the percentages of reliable voxels ($ICC \geq 0.4$) within each of the prior seven functional networks defined as in Fig. 1 are depicted as spider graphs.

the use of other experimental modalities (e.g., Deuker et al., 2009; MEG). This fact may be an indication of the many challenges that face large-scale parcellation-derived functional connectomes (Sporns, 2013), which will be discussed in next section.

4. Further considerations and future directions

As noted, both within- and between-subject variability can affect the level of test-retest reliability. Any factor that changes within- or between-subject variability thus possibly influences test-retest reliability. Meanwhile, the findings revealed by the meta-summary analysis implied that there are remarkable differences in test-retest reliability across different functional metrics and functional networks. It becomes a crucial point in developing a highly reliable method to investigate how the influential factors affect reliability and further reduce their impact by improving the current methodology for characterizing the human brain function. In this part, these factors are briefly reviewed, and some directions toward improvements on test-retest reliability of the current methods are discussed. Finally, the improvements are demonstrated based upon a set of high-quality multi-band RFMRI datasets from HCP (Smith et al., 2013a).

4.1. Factors interfering with test-retest reliability

Any variable or factor with significant intra- or inter-individual variability can influence test-retest reliability. As a demographic factor, age has been reproducibly shown to have significant effects on the human brain connectome regarding the voxel-wise functional metrics (e.g., Wu et al., 2007; Biswal et al., 2010; Zuo et al., 2010c, 2012; Tomasi and Volkow, 2012; Yang et al., 2012, 2014). Recently, it has been demonstrated to have a significant influence on the test-retest reliabilities of functional connectivity (Song et al., 2012). Moderate to substantial reliabilities have been

demonstrated within developing and aging populations (Thomason et al., 2011; Guo et al., 2012), calling for the need for establishing highly reliable computation methods or functional metrics across ages.

Physiological noise originating from respiration and cardiac processes impact iFC (Birn, 2012; Chang et al., 2009) and are potentially detrimental to the reliability of RFMRI measurements (Bright and Murphy, 2013a). Zuo and colleagues were the first to note that physiological noise can largely alter the estimation of amplitude measures of RFMRI signals (Zuo et al., 2010a). In that study, ALFF was demonstrated to have higher test-retest reliability than fALFF, but was more sensitive to physiological noise. From this perspective, fALFF should be recommended for use until an ideal method of reducing noise is developed. As a network metric, ICA has been demonstrated to have the ability of separating noisy components from RFMRI data (Beckmann, 2012). These noisy components were less test-retest reliable (Zuo et al., 2010b). Another factor, in-scanner head motion, exhibits large inter-individual variability. To demonstrate this inter-individual variability, we calculated the mean frame-wise displacement (Power et al., 2012, meanFD) of 234 healthy participants in the NCI Rockland Sample (NCI-RS) (Nooner et al., 2012), which is part of the INDI release. Fig. 6A depicted these individual differences in meanFD, indicating remarkable between-subject variability of the in-scanner head motion. These individual differences can have a large influence on various RFMRI measurements (Van Dijk et al., 2012; Satterthwaite et al., 2012, 2013; Bright and Murphy, 2013b; Mowinckel et al., 2012; Yan et al., 2013a; Tyskka et al., 2013; Power et al., 2013a, 2014), and also have significant influence on the reliability of RFMRI measures (Zuo et al., 2013; Yan et al., 2013a). It is very important to consider these factors when interpreting findings under common or, especially, more complicated experimental settings such as a day-cycle (Anderson et al., 2011b) or more long-term longitudinal changes. More physiological confounding factors in RFMRI have been discussed in a

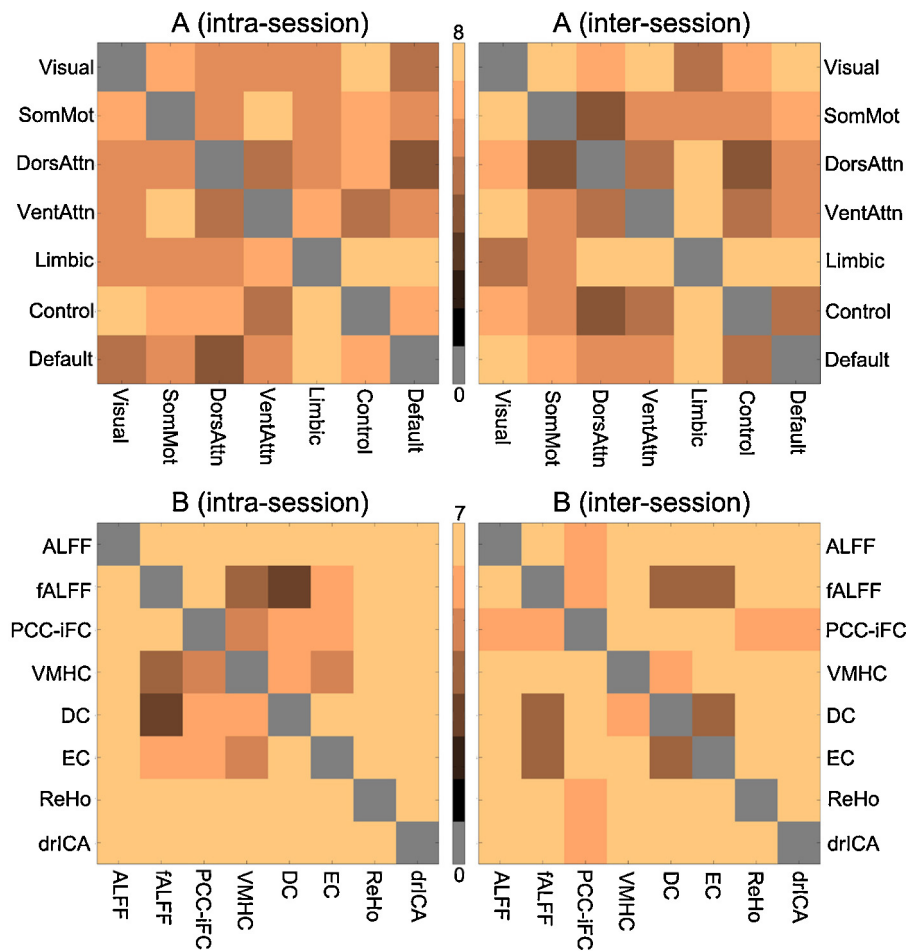


Fig. 5. Two-sample Kolmogorov-Smirnov (KS) tests on ICC distributions. To test whether the distributions of ICC values are significantly different between two networks or functional metrics, given one of the eight functional metrics (ALFF, fALFF, PCC-iFC, VMHC, DC, EC, ReHo, dRICA), we performed a two-sample KS test on the ICC values (Fisher-z transformed) of reliable voxels ($ICC \geq 0.4$) between each pair of the seven large-scale functional networks as defined in Fig. 1, resulting in a pair-wise KS significance matrix. Similarly, given each of the seven functional networks, we performed a two-sample KS test on the ICC values (Fisher-z transformed) of reliable voxels ($ICC \geq 0.4$) in this network between each pair of the eight functional metrics, leading to a pair-wise KS significance matrix. Any KS test on ICCs between network or metrics was determined as significant if its p -value was less than a critical p -value, which accounted for Bonferroni-based correction for multiple comparisons. The overlapping matrix A of the significances of comparisons was determined by summarizing pair-wise KS significance matrices across the eight metrics and visualized in the first row for both intra-session (~45 min) and inter-session (~6 months) test-retest reliabilities. The overlapping matrix B summarizes pair-wise KS significance matrices across the seven functional networks and is visualized in the second row.

recent review (Murphy et al., 2013) and their impacts on test-retest reliability require further systematic investigations.

Currently, different settings of ‘resting state’ are employed when performing an RFMRI experiment for data acquisition. One setting condition is the eye status (e.g., eyes-open, eyes-closed or fixation). Different settings can lead to differences in the mapping of functional connectome metrics and potentially reflect differences in neural correlates between these conditions (Yang et al., 2007; McAvoy et al., 2008; Zou et al., 2009; Yan et al., 2009; Liu et al., 2013b; Xu et al., 2014). How do they affect the test-retest reliability? This question has been increasingly recognized by the functional connectomics field. Recently, the influences of this factor on the test-retest reliability were comprehensively investigated by Patriat and colleagues (Patriat et al., 2013). The authors reported that the influences were relatively small in effect size but significant. Within-network connections were more reliable for default, attention, and auditory networks when the subjects were lying with their eyes fixated on a cross. In contrast, the primary visual network had most reliable connectivity when subjects kept their eyes open during the scanning.

Scan length during RFMRI experiments is another factor recognized to have significant effects on the functional connectomics

(Van Dijk et al., 2010). Zuo and colleagues demonstrated that a longer scanning duration can gain in test-retest reliability of the functional homogeneity metric (Zuo et al., 2013), although a 5-min RFMRI scan was sufficient to achieve 50% reliability, which has recently been replicated for network centrality metrics (Liao et al., 2013). This effect was further investigated in a recent reliability study on functional connectivity (Birn et al., 2013) by examining the test-retest reliability for RFMRI scans ranging in length from 3 to 27 min. Basically, reliability can be greatly improved by increasing the scan lengths from 5 min to 13 min. This gain in reliability from the increased scan length is substantially greater for intra-session scans, whereas that in the inter-session reliability diminished after 9–12 min.

While some factors such as physiological noise and scan duration have been evaluated with regard to their impact on test-retest reliability, other factors remain to be investigated with regard to their influences on reliability. For instance, the quality of brain image registration can exhibit large and remarkable inter-individual variability, and thus potentially affect test-retest reliability. To demonstrate the inter-individual variability of registration, we employed the NKI-RS large sample ($N=234$), which was acquired at a single site. Fig. 6 visualizes the inter-individual

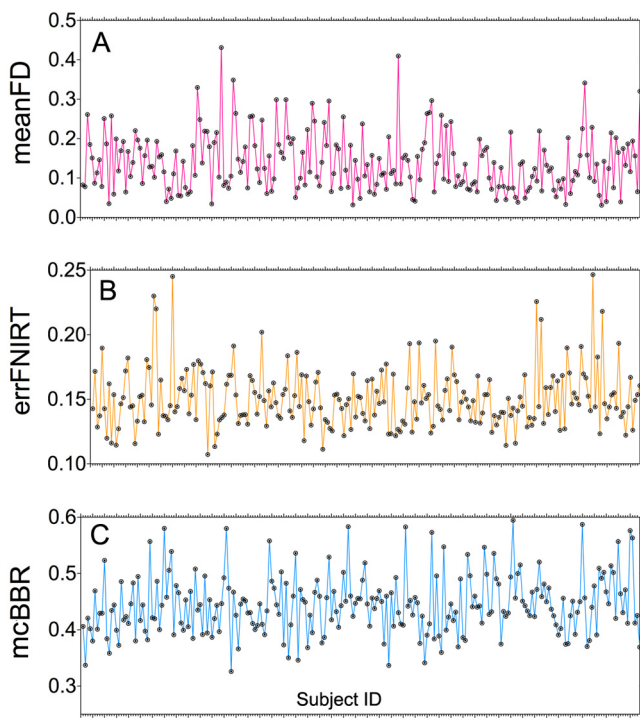


Fig. 6. Individual differences in in-scanner head motion and image registration quality. The RFMRI datasets of total 234 subjects were adopted from the NKI-Rockland sample in the International Neuroimaging Data-Sharing Initiative (INDI) (fcon_1000.projects.nitrc.org/indi). For each subject, (A) the error of nonlinear registration using FNIRT (errFNIRT), (B) the minimal cost of function–structure realignment using boundary-based registration (mCBRR), and (C) the mean frame-wise displacement (meanFD) were estimated and plotted. The x-axis indicates the subject. Details of these quantities can be found at the webpage for quality control procedure in Connectome Computation System (CCS: lfcd.psych.ac.cn/ccs/QC.html).

variabilities of registration quality measures (Jiang et al., 2014) (lfcd.psych.ac.cn/ccs/QC.html) of both nonlinear (Fig. 6B) and linear (Fig. 6C) registrations across the 234 NKR-RS subjects. The quality of the nonlinear registration was quantified with spatial correlation between the registered individual image and the MNI152 standard template (Zuo et al., 2010c), whereas the minimal cost of function–structure realignment using boundary-based registration (mCBRR) was used to quantify the linear registration quality (Greve and Fischl, 2009). It is completely unknown whether and how this registration-related factor significantly affects the test-retest reliabilities of common RFMRI measurements; therefore, it deserves to be carefully examined in future functional connectomics studies.

4.2. Improving reliability in functional connectomics

New techniques that improve test-retest reliability across physiological noise, sessions and eye conditions as well as various processing choices will be critical for guiding the interpretation of functional connectomics studies. A promising direction to improve reliability is data processing and standardization strategies (Yan et al., 2013b), which should be comprehensively investigated with regard to their effects on the test-retest reliabilities of mapping human functional connectomes. Efforts have been made to improve the test-retest reliabilities of functional connectome measures toward this direction. Many data processing factors including global signal regression, spatial/temporal smoothing and computational space (i.e., volume versus surface), and others have been proposed to address physiological noise and other inter-individual variability. Spatially smoothing higher resolution fMRI data improve temporal SNR beyond that of data originally acquired

at a lower resolution, however, the advantage of resolution accuracy in space is lost. Molloy et al. (2014) found that there were no significant differences in functional connectivity as a function of resolution after Gaussian spatial smoothing. However, the advancements in image de-noising algorithms such as non-local means spatial smoothing has been demonstrated to improve the reliability of default network connectivity mapping (Zuo and Xing, 2011; Xing et al., 2013) without hurting the intrinsic data resolution. The commonly used Gaussian smoothing has been investigated to reduce test-retest reliability of local functional homogeneity (Zuo et al., 2013). The use of global signal regression (GSR) also lowers the test-retest reliability of local functional homogeneity (Zuo et al., 2013) whereas GSR seemed to show negligible effect on ICC of language network iFC (Zhu et al., 2014). Such a controversial pre-processing step (Fox et al., 2009; Murphy et al., 2009) has been comprehensively investigated as an individual-level standardization of the intrinsic brain (Yan et al., 2013b). More reasonable image preprocessing techniques, long scan durations, high imaging resolutions and well-designed computational strategies can significantly increase test-retest reliability, for example, volume vs. surface (Zuo et al., 2013), wavelet vs. Pearson correlation (Wang et al., 2013a) and parameters selection in use of data-driven algorithms (e.g., Poppe et al., 2013, ICA). Development of novel metrics to achieve more accurate estimations of different aspects of reliability are also in progress (e.g., Shou et al., 2014, image-based ICC evaluation).

Graph theory-based functional connectomics had only moderate test-retest reliability as demonstrated in the previous section. This does not necessarily suggest that the graph theory has no great value in the functional connectomics but may rather reflect the many challenges of defining a reliable graph for the human brain function at this stage. As one example of these challenges, defining a node based on a large structural/anatomical region and building an edge for a brain graph can be problematic. Simply averaging the voxel-wise time series from a large region ignores the fact that the strength of functional homogeneity within large structural areas is typically low and highly variable across spatial locations, which leads to difficulties in the interpretation of the mean time series and derived connectome metrics and artificial alterations of both within- and between-subjects variability causing low test-retest reliability. The high degree of regional variation in local functional homogeneity (Zuo et al., 2013) challenges the predefined brain parcellation strategies and requires more sophisticated brain parcellations that consider regional variation and inter-individual variability in both the structure and function of the human brain at the group and individual levels (Blumensath et al., 2013; Wig et al., 2013; Jiang et al., 2014). One fundamental factor in voxel-wise functional connectivity graphs (VFCGs) is the edge density, which is defined as the proportion of actual edges in all possible edges for a graph. There is no gold standard on what level of edge density of a brain graph should be. Most previous studies reported edge densities between 1% to 10%, leading to a sparse graph. Thus, the edge density sometime was also called ‘sparsity’. Most recent studies on monkeys revealed that the edge density of the anatomical or structural brain connectome can be very high (>60%), resulting in a highly connected graph (Markov et al., 2014, 2013; Ercsey-Ravasz et al., 2013). For the human brain, limited by the brain mapping technology, it remains challenging to achieve an anatomical or a structural connectome at voxel level currently. However, it has been well recognized that VFCGs are based on and shaped by their structural connectomes (Honey et al., 2007), which is highly test-retest reliable and reproducible. Mapping the most reliable VFCGs across different edge densities becomes an indirect way of mapping structural connectomes at the voxel level for human. The low ICCs of VFCGs observed in the present study may be just an indication that the edge densities of the VFCGs are not optimal to reliability.

The successful construction of individual-level brain functional parcellation techniques will not only produce more reliable functional connectome metrics but also advance the development of personalized treatments such as more precise positioning for brain surgery. In future studies, a good standard for RFMRI data analysis and RFMRI protocols as well as for choosing optimal edge density of VFCGs should be established for functional connectomics in terms of a requirement of high test-retest reliability for the development of RFMRI-based biological tests in the clinic.

In the last part of this section, we aim to show improvements in reliability by addressing the factors discussed above based upon the preprocessed datasets acquired with advanced RFMRI sequences (Moeller et al., 2010; Feinberg et al., 2010) from 80 unrelated healthy subjects in the HCP Q3 release database (Van Essen et al., 2013; Smith et al., 2013a; Glasser et al., 2013). The details of these data can be found in HCP Q3 Release Reference Manual (www.humanconnectome.org/documentation/Q3). Here, we only provide certain key data features and processing steps that could potentially contribute to reliability improvements. Specifically, each HCP subject underwent 1 h of whole-brain RFMRI scanning acquired with two pairs of 15-min runs in two days and thus had four 15-min RFMRI scans (3 retest scans). A spatial resolution of 2-mm voxel and a temporal resolution of 0.7 s were achieved with a multi-band EPI acceleration factor of 8. All subjects were instructed to lie with their eyes open, with 'relaxed' fixation on a white cross (on a dark background), think of nothing in particular, and not fall asleep. To address the registration error and related inter-individual variability discussed above, HCP has put significant effort into minimizing MRI spatial distortion and signal loss and obtaining an accurate registration of the RFMRI images to the high-resolution (0.7-mm isotropic voxel) structural image of each subject. This allows for the transformation of the cortical RFMRI signal from the originally acquired 3D voxel matrix onto a gray matter surface mesh. Surface-based analysis represents gray matter with a better respect to its natural geometry and therefore allows for better functional alignment across subjects (Van Essen and Dierker, 2007) and improvements of reliability (e.g., Zuo et al., 2013). The minimally preprocessed individual RFMRI timeseries are transferred from native surface meshes to the Conte69 32k template mesh (2 mm average vertex spacing, total 32,494 vertices per hemisphere) (Van Essen et al., 2012) and further smoothed (2 mm FWHM) on the surface (Smith et al., 2013a). Several efforts have also been made to address various noisy confounds in RFMRI data of the HCP Q3 release. A minimal high-pass filtering with a 2000s FWHM was applied, which was similar to the removal of linear trends from the data. The 24 confound time series derived from the motion estimation were regressed out of the data (Yan et al., 2013a; Satterthwaite et al., 2013). FIX (FMRIB's ICA-based X-noisifier) was applied to classify RFMRI data components in the volume space into 'good' vs. 'bad' (Salimi-Khorshidi et al., 2014). Bad components identified as artifactual processes by FIX were then removed from the RFMRI data in the surface space.

With these ICA FIXed RFMRI datasets (total 320 scans), we computed six of the eight functional metrics (i.e., ALFF, fALFF, ReHo, VMHC, DC, EC) for each vertex on the Conte69 32k cortical surface. Of note, both seed-based iFC and ICA have been extensively evaluated with the HCP datasets in several recent studies (Smith et al., 2013a,b; Yeo et al., 2013), and thus not included. This resulted in the surface version vertex-wise maps of previous voxel-wise maps of these metrics (Zuo et al., 2010a,c, 2012, 2013). In relation to the previous studies, there were several changes of analytic strategy worth to be mentioned here. First, there was no any explicit temporal low-pass filtering operation in preprocessing the HCP data regarding recent evidence on the presence of high-frequency neuronal-related RFMRI signal (Feinberg et al., 2010).

Second, a small spatial smoothing (FWHM = 2 mm) on the surface was performed. Accordingly, we expanded the neighbor size in ReHo computation to 4 mm (i.e., averagely two times of the distance between two adjacent vertices on the surface) to reduce the effects of smoothing (Zuo et al., 2013). Finally, to make these large vertex-wise brain graphs (59,369 nodes) more comparable across individuals and scans (Bullmore and Bassett, 2011), we threshed these full correlation matrices (59,369 × 59,369) to have the same edge density of 5% (about 850M edges) for estimation of both DC and EC. Of note, the weighted graphs were used for preservation of more information of functional connectivity (Zuo et al., 2012; Turk-Browne, 2013).

To rule out the effect of multi-band RFMRI phase-coding direction in reliability analysis, we used the individual mean maps of each functional metrics across one day to evaluate the two-day inter-session test-retest reliability with the statistical model described in prior. Specifically, for each metric ϕ_{ij}^m both global mean $gm\Phi_{ij}^m$ and standard deviation (log transformed) $\log(gsd\Phi_{ij}^m)$ of each functional metric were modeled as scan-level covariates (Yan et al., 2013b). Here, $1 \leq m \leq 6$, $1 \leq i \leq 2$, and $1 \leq j \leq 80$ were the labels for metrics, sessions and participants). At each vertex v , a statistical model (7) is set up for estimating the mean and ICC of this metric across the 80 participants.

$$\phi_{ij}^m(v) = \lambda_{0j}(v) + gm\Phi_{ij}^m + \log(gsd\Phi_{ij}^m) + e_{ij}; \lambda_{0j}(v) = \mu_{00}(v) + p_{0j}(v) \quad (7)$$

where μ_{00} is a fixed parameter (the group mean) and p_{0j} and e_{ij} are independent random effects normally distributed with mean 0 and variances σ_p^2 and σ_e^2 . The term p_{0j} is the participant effect and e_{ij} is the measurement error. The ICC is then estimated with Eq. (5). This exploration revealed a striking improvement of ICC for substantial to almost perfect test-retest reliability (ICC ≥ 0.6) of ReHo, ALFF, fALFF, and VMHC across the entire cortex (Fig. 7), whereas the meta-summary reliability analysis on these vertex-wise ICC maps led to similar findings to the previous analyses (data not shown). Of note, both amplitude metrics (ALFF and fALFF) exhibited very high inter-session reliability. In contrast to the previous findings (Zuo et al., 2010a), this observation is likely an indication of the improvement on the RFMRI data quality. Again, both graph theory metrics (DC and EC) had the lowest test-retest reliabilities among the six metrics.

4.3. Call for consortium for reliability and reproducibility

The challenges of reliability and reproducibility of scientific findings have been increasingly recognized (Russell, 2013; Editorials, 2013). In functional connectomics, although promising for specific data (e.g., HCP), the factors interfering with reliability and reproducibility as well as their interactions remain largely unidentified due to the lack of a large-scale, retest condition-rich data for evaluating potential factors. Even when based on small samples, test-retest data and the corresponding estimations of test-retest reliabilities could strengthen the application of relevant findings (e.g., Di Martino et al., 2009; Zuo et al., 2010c; Zhao et al., 2013; Peng et al., 2014). However, the available studies based on small samples of test-retest RFMRI data will be statistically powered with a large test-retest sample. A generation of openly available large-sample multimodal test-retest neuroimaging datasets would be extremely valuable for the imaging community. This dataset source would facilitate the establishment of the test-retest reliabilities of commonly-used MR-based metrics of connectomes, the determination of the ranges of variation in the reliabilities of these metrics across imaging sites and/or retest study designs, and the creation of a standard benchmark dataset

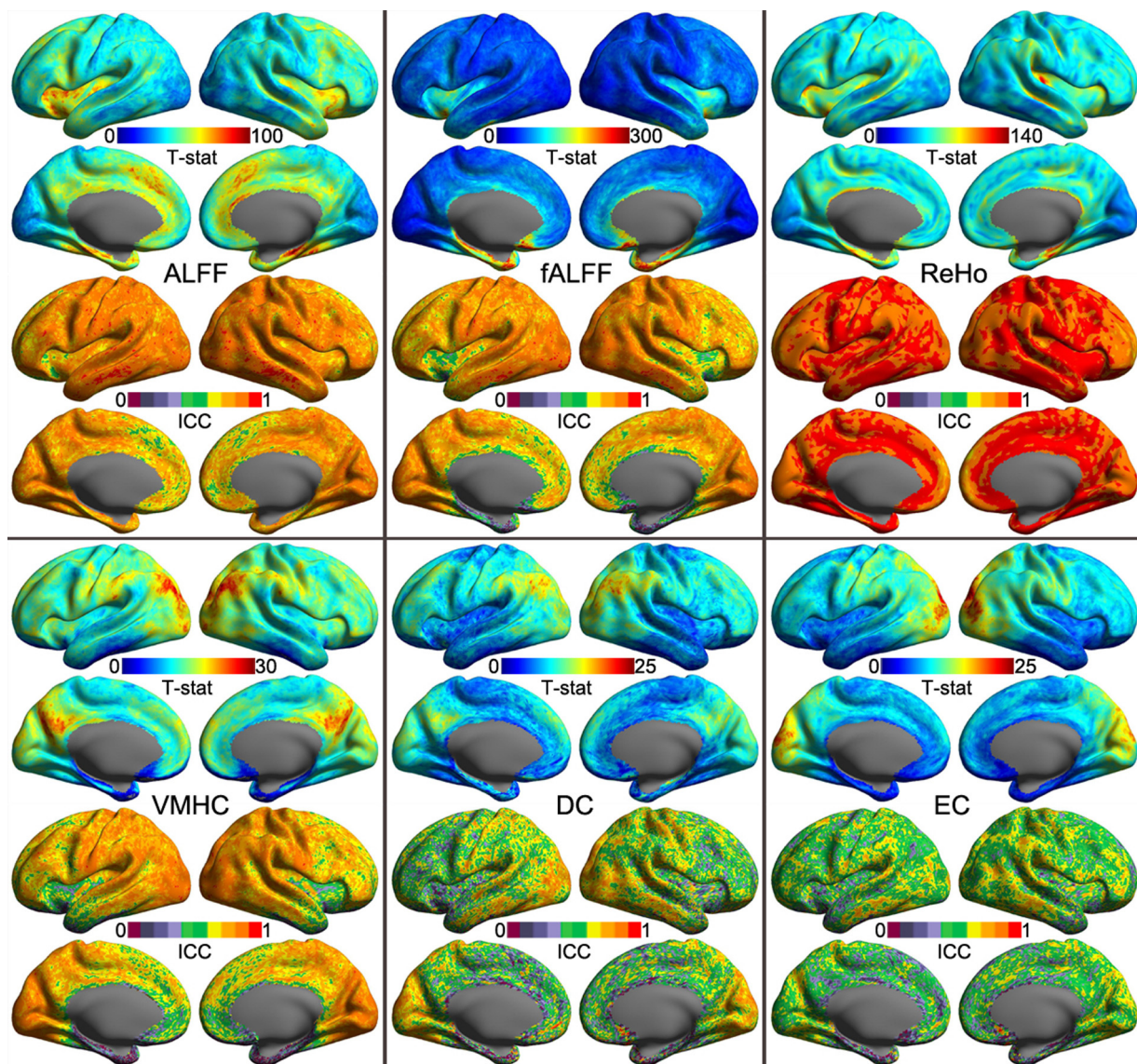


Fig. 7. Test-retest reliability of functional connectome metrics for HCP Q3 release RFMRI data. On the cortical surface (32,492 surface nodes or vertices) defined by the Conte69 human surface-based atlas (Conte69.32k), six functional connectome metrics (ALFF, fALFF, ReHo, VMHC, DC, EC) were estimated for each of 320 individual multi-band RFMRI scans ($TR = 700$ ms) from 80 unrelated participants (each had 4 test-retest RFMRI scans in two days) as part of the Human Connectome Project (HCP) Q3 release. Given a functional metric, a linear mixed model based on all 320 individual vertex-wise metric maps generated both vertex-wise group-level mean (i.e., the T -statistics) and vertex-wise inter-session ICC maps of the functional metric on the cortical surface. These vertex-wise maps are depicted onto the Conte69.32k cortical surfaces.

for the evaluation of novel metrics. To achieve this objective, a new grassroots effort has been initiated via the Consortium for Reliability and Reproducibility (CoRR) by Prof. Xi-Nian Zuo and Dr. Michael Peter Milham. Although still in progress, CoRR has been supported by more than 30 international sites to share test-retest multimodal neuroimaging datasets from more than 1500 healthy people (http://fcon_1000.projects.nitrc.org/indi/CoRR/html/index.html)

5. Conclusions and recommendations

The overall spatial pattern of common RFMRI measurements can be reliably detected across different times and large-scale networks. The regional variations of test-retest reliability of various RFMRI metrics are reflected at the network level across the common seven large-scale neural networks, among which, the high-order associative networks have the highest reliability, whereas the limbic network exhibits the lowest reliability.

The voxel-wise metrics of functional connectomes can exhibit high-level regional variations with moderate to almost perfect test-retest reliabilities across large-scale neural systems. These variations likely reflect both stable and dynamic aspects of the intrinsic architecture of the human functional connectome. Among the metrics examined, local functional homogeneity with anatomical constraints and intrinsic functional connectivity derived by independent component analysis with dual regression as well as functional homotopy are the three metrics with the greatest reliability. Amplitude metrics and their test-retest reliabilities appeared highly dependent on the data quality. An openly available source of large-sample, multimodal, test-retest neuroimaging datasets is required to identify various factors interfering with reliability and to produce well-designed data acquisition, preprocessing and analysis standards that can account for both inter- and intra-individual variability in the macro-scale human brain connectomics.

In light of the review on previous findings and discussions in prior, we recommend the use of functional connectomics at the current stage with:

- The instruction of eyes-open with fixation during RFMRI scans.
- The setting of a longer duration (6–15 min) for RFMRI scans.
- The acceleration of EPI sequences for high tempo-spatial resolution.
- The strategy of two-dimensional surface-based processing and analysis.
- The use of ICA, ReHo and VMHC functional connectivity metrics.
- The examination of default, control and attention networks.

Funding

Dr. Xi-Nian Zuo acknowledges the funding support from the Hundred Talents Program, the Key Research Program (KSZD-EWTZ-002) of the Chinese Academy of Sciences, the Major Joint Fund for International Cooperation and Exchange of the National Natural Science Foundation (81220108014). Dr. Xiu-Xia Xing's research is supported by the Fundamental Development Program on Mathematics and Statistics from Beijing University of Technology and the Natural Science Foundation of China (81201153). RFMRI data were provided by the HCP WU-Minn Consortium, which is funded by the 16 NIH institutes and centers that support the NIH Blueprint for Neuroscience Research 1U54MH091657 (PIs: David Van Essen and Kamil Ugurbil), the McDonnell Center for Systems Neuroscience at Washington University, and the INDI NKI-RS project, which is supported by the NIMH BRAINS program R01MH094639-01 (PI: Michael Peter Milham).

Conflict of interest statement

The authors declare that the research was conducted in the absence of any commercial or financial relationships that could be construed as a potential conflict of interest.

Acknowledgments

Dr. Xi-Nian Zuo is indebted to Yu-Feng Zang, Michael Peter Milham and F. Xavier Castellanos, who introduced him to open neuroscience with RFMRI and have provided endless supports. Without their encouragement and comments, this review would not have been possible. We thank Zarrar Shehzad and Chao-Gan Yan for sharing their reliability maps, Donna Dierker for discussions about the design and implementation of surface-based cortical analyses with the RFMRI data from the HCP Q3 release, Yong He and Olaf Sporns for their insightful comments on graph-based connectomics, Ting Xu for the assistance in statistical models and computation of the test-retest reliability, and Zhe Zhang, Ye He and Bing Chen for references collection.

References

- Achard, S., Salvador, R., Whitcher, B., Suckling, J., Bullmore, E., 2006. A resilient, low-frequency, small-world human brain functional network with highly connected association cortical hubs. *J. Neurosci.* **26** (1), 63–72.
- Adelstein, J.S., Shehzad, Z., Mennes, M., Deyoung, C.G., Zuo, X.N., Kelly, C., Margulies, D.S., Bloomfield, A., Gray, J.R., Castellanos, F.X., Milham, M.P., 2011. Personality is reflected in the brain's intrinsic functional architecture. *PLoS One* **6** (11), e27633.
- Akil, H., Martone, M.E., Van Essen, D.C., 2011. Challenges and opportunities in mining neuroscience data. *Science* **331** (6018), 708–812.
- Albert, N.B., Robertson, E.M., Miall, R.C., 2009. The resting human brain and motor learning. *Curr. Biol.* **19** (12), 1023–1027.
- Alivisatos, A.P., Andrews, A.M., Boyden, E.S., Chun, M., Church, G.M., Deisseroth, K., Donoghue, J.P., Fraser, S.E., Lippincott-Schwartz, J., Looger, L.L., Masmanidis, S., McEuen, P.L., Nurmikko, A.V., Park, H., Peterka, D.S., Reid, C., Roukes, M.L., Scherer, A., Schnitzer, M., Sejnowski, T.J., Shepard, K.L., Tsao, D., Turrigiano, G., Weiss, P.S., Xu, C., Yuste, R., Zhuang, X., 2013a. Nanotools for neuroscience and brain activity mapping. *ACS Nano* **7** (3), 1850–1866.
- Alivisatos, A.P., Chun, M., Church, G.M., Deisseroth, K., Donoghue, J.P., Greenspan, R.J., McEuen, P.L., Roukes, M.L., Sejnowski, T.J., Weiss, P.S., Yuste, R., 2013b. Neuroscience, the brain activity map. *Science* **339** (6125), 1284–1285.
- Alivisatos, A.P., Chun, M., Church, G.M., Greenspan, R.J., Roukes, M.L., Yuste, R., 2012. The brain activity map project and the challenge of functional connectomics. *Neuron* **74** (6), 970–974.
- Allen, E.A., Damaraju, E., Plis, S.M., Erhardt, E.B., Eichele, T., Calhoun, V.D., 2014. Tracking whole-brain connectivity dynamics in the resting state. *Cereb. Cortex* **24**, 663–676.
- Anderson, J.S., Druzgal, T.J., Froehlich, A., DuBray, M.B., Lange, N., Alexander, A.L., Abildskov, T., Nielsen, J.A., Cariello, A.N., Cooperider, J.R., Bigler, E.D., Lainhart, J.E., 2011a. Decreased interhemispheric functional connectivity in autism. *Cereb. Cortex* **21** (5), 1134–1146.
- Anderson, J.S., Ferguson, M.A., Lopez-Larson, M., Yurgelun-Todd, D., 2011b. Reproducibility of single-subject functional connectivity measurements. *AJNR Am. J. Neuroradiol.* **32** (3), 548–555.
- Anderson, J.S., Zielinski, B.A., Nielsen, J.A., Ferguson, M.A., 2014. Complexity of low-frequency blood oxygen level-dependent fluctuations covaries with local connectivity. *Hum. Brain Map.* **35** (4), 1273–1283.
- Barnhart, H.X., Haber, M.J., Lin, L.I., 2007. An overview on assessing agreement with continuous measurements. *J. Biopharm. Stat.* **17** (4), 529–569.
- Bassett, D.S., Wymbs, N.F., Porter, M.A., Mucha, P.J., Carlson, J.M., Grafton, S.T., 2011. Dynamic reconfiguration of human brain networks during learning. *Proc. Natl. Acad. Sci. U. S. A.* **108** (18), 7641–7646.
- Beckmann, C.F., 2012. Modelling with independent components. *Neuroimage* **62** (2), 891–901.
- Beckmann, C.F., DeLuca, M., Devlin, J.T., Smith, S.M., 2005. Investigations into resting-state connectivity using independent component analysis. *Philos. Trans. R. Soc. Lond. B Biol. Sci.* **360** (1457), 1001–1013.
- Bellec, P., Rosa-Neto, P., Lyttelton, O.C., Benali, H., Evans, A.C., 2010. Multi-level bootstrap analysis of stable clusters in resting-state fMRI. *Neuroimage* **51** (3), 1126–1139.
- Bernal-Rusiel, J.L., Greve, D.N., Reuter, M., Fischl, B., Sabuncu, M.R., 2012. Alzheimer's Disease Neuroimaging I. Statistical analysis of longitudinal neuroimage data with linear mixed effects models. *Neuroimage* **66C**, 249–260.
- Bernal-Rusiel, J.L., Reuter, M., Greve, D.N., Fischl, B., Sabuncu, M.R., 2013. Alzheimer's disease neuroimaging. I. Spatiotemporal linear mixed effects modeling for the mass-univariate analysis of longitudinal neuroimage data. *Neuroimage* **81**, 358–370.
- Birn, R.M., 2012. The role of physiological noise in resting-state functional connectivity. *Neuroimage* **62** (2), 864–870.
- Birn, R.M., Molloy, E.K., Patriat, R., Parker, T., Meier, T.B., Kirk, G.R., Nair, V.A., Meyerand, M.E., Prabhakaran, V., 2013. The effect of scan length on the reliability of resting-state fMRI connectivity estimates. *Neuroimage* **83C**, 550–558.
- Birn, R.M., Smith, M.A., Jones, T.B., Bandettini, P.A., 2008. The respiration response function: the temporal dynamics of fMRI signal fluctuations related to changes in respiration. *Neuroimage* **40** (2), 644–654.
- Biswal, B., Yetkin, F.Z., Haughton, V.M., Hyde, J.S., 1995. Functional connectivity in the motor cortex of resting human brain using echo-planar MRI. *Magn. Reson. Med.* **34** (4), 537–541.
- Biswal, B.B., Mennes, M., Zuo, X.N., Gohel, S., Kelly, C., Smith, S.M., Beckmann, C.F., Adelstein, J.S., Buckner, R.L., Colcombe, S., Dogonowski, A.M., Ernst, M., Fair, D., Hampson, M., Hoptman, M.J., Hyde, J.S., Kiviniemi, V.J., Kotter, R., Li, S.J., Lin, C.P., Lowe, M.J., Mackay, C., Madden, D.J., Madsen, K.H., Margulies, D.S., Mayberg, H.S., McMahon, K., Monk, C.S., Mostofsky, S.H., Nagel, B.J., Pekar, J.J., Peltier, S.J., Petersen, S.E., Riedl, V., Rombouts, S.A., Rympa, B., Schlaggar, B.L., Schmidt, S., Seidler, R.D., Siegle, G.J., Sorg, C., Teng, G.J., Veijola, J., Villringer, A., Walter, M., Wang, L., Weng, X.C., Whitfield-Gabrieli, S., Williamson, P., Windischberger, C., Zang, Y.F., Zhang, H.Y., Castellanos, F.X., Milham, M.P., 2010. Toward discovery science of human brain function. *Proc. Natl. Acad. Sci. U. S. A.* **107** (10), 4734–4739.
- Blumenthal, T., Jbabdi, S., Glasser, M.F., Van Essen, D.C., Ugurbil, K., Behrens, T.E., Smith, S.M., 2013. Spatially constrained hierarchical parcellation of the brain with resting-state fMRI. *Neuroimage* **76**, 313–324.
- Braun, U., Plichta, M.M., Esslinger, C., Sauer, C., Haddad, L., Grimm, O., Mier, D., Mohnke, S., Heinz, A., Erk, S., Walter, H., Seiferth, N., Kirsch, P., Meyer-Lindenberg, A., 2012. Test-retest reliability of resting-state connectivity network characteristics using fMRI and graph theoretical measures. *Neuroimage* **59** (2), 1404–1412.
- Bright, M.G., Murphy, K., 2013a. Reliable quantification of BOLD fMRI cerebrovascular reactivity despite poor breath-hold performance. *Neuroimage* **83C**, 559–568.
- Bright, M.G., Murphy, K., 2013b. Removing motion and physiological artifacts from intrinsic BOLD fluctuations using short echo data. *Neuroimage* **64**, 526–537.
- Broyd, S.J., Demanuele, C., Debener, S., Helps, S.K., James, C.J., Sonuga-Barke, E.J., 2009. Default-mode brain dysfunction in mental disorders: a systematic review. *Neurosci. Biobehav. Rev.* **33** (3), 279–296.
- Buckner, R.L., 2012. The serendipitous discovery of the brain's default network. *Neuroimage* **62** (2), 1137–1145.
- Buckner, R.L., Krienen, F.M., Castellanos, A., Diaz, J.C., Yeo, B.T., 2011. The organization of the human cerebellum estimated by intrinsic functional connectivity. *J. Neurophysiol.* **106** (5), 2322–2345.
- Buckner, R.L., Krienen, F.M., Yeo, B.T., 2013. Opportunities and limitations of intrinsic functional connectivity MRI. *Nat. Neurosci.* **16** (7), 832–837.
- Buckner, R.L., Sepulcre, J., Talukdar, T., Krienen, F.M., Liu, H., Hedden, T., Andrews-Hanna, J.R., Sperling, R.A., Johnson, K.A., 2009. Cortical hubs revealed by intrinsic

- functional connectivity: mapping, assessment of stability, and relation to Alzheimer's disease.** *J. Neurosci.* 29 (6), 1860–1873.
- Buckner, R.L., Snyder, A.Z., Shannon, B.J., LaRossa, G., Sachs, R., Fotenos, A.F., Sheeline, Y.I., Klunk, W.E., Mathis, C.A., Morris, J.C., Mintun, M.A., 2005. Molecular, structural, and functional characterization of Alzheimer's disease: evidence for a relationship between default activity, amyloid, and memory. *J. Neurosci.* 25 (34), 7709–7717.
- Bullmore, E., Sporns, O., 2009. Complex brain networks: graph theoretical analysis of structural and functional systems. *Nat. Rev. Neurosci.* 10 (3), 186–198.
- Bullmore, E., Sporns, O., 2012. The economy of brain network organization. *Nat. Rev. Neurosci.* 13 (5), 336–349.
- Bullmore, E.T., Bassett, D.S., 2011. Brain graphs: graphical models of the human brain connectome. *Annu. Rev. Clin. Psychol.* 7, 113–140.
- Buzsaki, G., Draguhn, A., 2004. Neuronal oscillations in cortical networks. *Science* 304 (5679), 1926–1929.
- Cao, M., Wang, J.H., Dai, Z.J., Cao, X.Y., Jiang, L.L., Fan, F.M., Song, X.W., Xia, M.R., Shu, N., Dong, Q., Milham, M.P., Castellanos, F.X., Zuo, X.N., He, Y., 2014. Topological organization of the human brain functional connectome across the lifespan. *Dev. Cogn. Neurosci.* 7, 76–93.
- Carmines, E., Zeller, R., 1979. Reliability and Validity Assessment. Number no. 17 in 07. SAGE Publications.
- Castellanos, F.X., Di Martino, A., Craddock, R.C., Mehta, A.D., Milham, M.P., 2013. Clinical applications of the functional connectome. *Neuroimage* 80, 527–540.
- Chang, C., Cunningham, J.P., Glover, G.H., 2009. Influence of heart rate on the BOLD signal: the cardiac response function. *Neuroimage* 44 (3), 857–869.
- Chang, C., Glover, G.H., 2009a. Effects of model-based physiological noise correction on default mode network anti-correlations and correlations. *Neuroimage* 47 (4), 1448–1459.
- Chang, C., Glover, G.H., 2009b. Relationship between respiration, end-tidal CO₂, and BOLD signals in resting-state fMRI. *Neuroimage* 47 (4), 1381–1393.
- Chen, G., Saad, Z.S., Britton, J.C., Pine, D.S., Cox, R.W., 2013. Linear mixed-effects modeling approach to fMRI group analysis. *Neuroimage* 73, 176–190.
- Choi, E.Y., Yeo, B.T., Buckner, R.L., 2012. The organization of the human striatum estimated by intrinsic functional connectivity. *J. Neurophysiol.* 108 (8), 2242–2263.
- Cole, D.M., Smith, S.M., Beckmann, C.F., 2010. Advances and pitfalls in the analysis and interpretation of resting-state fMRI data. *Front. Syst. Neurosci.* 4, 8.
- Cordes, D., Haughton, V., Carew, J.D., Arfanakis, K., Maravilla, K., 2002. Hierarchical clustering to measure connectivity in fMRI resting-state data. *Magn. Reson. Imaging* 20 (4), 305–317.
- Cox, R.W., 2012. AFNI: what a long strange trip it's been. *Neuroimage* 62 (2), 743–747.
- Craddock, R.C., Jbabdi, S., Yan, C.G., Vogelstein, J.T., Castellanos, F.X., Di Martino, A., Kelly, C., Heberlein, K., Colcombe, S., Milham, M.P., 2013. Imaging human connectomes at the macroscale. *Nat. Methods* 10 (6), 524–539.
- Deco, G., Corbetta, M., 2011. The dynamical balance of the brain at rest. *Neuroscientist* 17 (1), 107–123.
- Deco, G., Jirsa, V.K., McIntosh, A.R., 2011. Emerging concepts for the dynamical organization of resting-state activity in the brain. *Nat. Rev. Neurosci.* 12 (1), 43–56.
- Deco, G., Ponce-Alvarez, A., Mantini, D., Romani, G.L., Hagmann, P., Corbetta, M., 2013. Resting-state functional connectivity emerges from structurally and dynamically shaped slow linear fluctuations. *J. Neurosci.* 33 (27), 11239–11252.
- Deshpande, G., LaConte, S., Peltier, S., Hu, X., 2009. Integrated local correlation: a new measure of local coherence in fMRI data. *Hum. Brain Map.* 30 (1), 13–23.
- Deuker, L., Bullmore, E.T., Smith, M., Christensen, S., Nathan, P.J., Rockstroh, B., Bassett, D.S., 2009. Reproducibility of graph metrics of human brain functional networks. *Neuroimage* 47 (4), 1460–1468.
- Di Martino, A., Shehzad, Z., Kelly, C., Roy, A.K., Gee, D.G., Uddin, L.Q., Gotimer, K., Klein, D.F., Castellanos, F.X., Milham, M.P., 2009. Relationship between cingulo-insular functional connectivity and autistic traits in neurotypical adults. *Am. J. Psychiatry* 166 (8), 891–899.
- Di Martino, A., Yan, C.G., Li, Q., Denio, E., Castellanos, F.X., Alaerts, K., Anderson, J.S., Assaf, M., Bookheimer, S.Y., Dapretto, M., Deen, B., Delmonte, S., Dinstein, I., Ertl-Wagner, B., Fair, D.A., Gallagher, L., Kennedy, D.P., Keown, C.L., Keysers, C., Lainhart, J.E., Lord, C., Luna, B., Menon, V., Minshew, N.J., Monk, C.S., Mueller, S., Muller, R.A., Nebel, M.B., Nigg, J.T., O'Hearn, K., Pelpfrey, K.A., Peltier, S.J., Rudie, J.D., Sunaert, S., Thioux, M., Tyszka, J.M., Uddin, L.Q., Verhoeven, J.S., Wenderoth, N., Wiggins, J.L., Mostofsky, S.H., Milham, M.P., 2014. The autism brain imaging data exchange: towards a large-scale evaluation of the intrinsic brain architecture in autism. *Mol. Psychiatry* 19 (6), 659–667.
- Dong, M., Qin, W., Zhao, L., Yang, X., Yuan, K., Zeng, F., Sun, J., Yu, D., von Deneen, K.M., Liang, F., Tian, J., 2014. Expertise modulates local regional homogeneity of spontaneous brain activity in the resting brain: An fMRI study using the model of skilled acupuncturists. *Hum. Brain Map.* 35 (3), 1074–1084.
- Dosenbach, N.U.F., Nardos, B., Cohen, A.L., Fair, D.A., Power, J.D., Church, J.A., Nelson, S.M., Wig, G.S., Vogel, A.C., Lessov-Schlaggar, C.N., Barnes, K.A., Dubis, J.W., Feczkó, E., Coalson, R.S., Prueitt, J.R., Barch, D.M., Petersen, S.E., Schlaggar, B., 2010. Prediction of individual brain maturity using fMRI. *Science* 329 (5997), 1358–1361.
- Editorials, 2013. Reducing our irreproducibility. *Nature* 496 (7446), 398.
- Ercsey-Ravasz, M., Markov, N.T., Lamy, C., Van Essen, D.C., Knoblauch, K., Toroczkai, Z., Kennedy, H., 2013. A predictive network model of cerebral cortical connectivity based on a distance rule. *Neuron* 80 (1), 184–197.
- Erhardt, E.B., Rachakonda, S., Bedrick, E.J., Allen, E.A., Adali, T., Calhoun, V.D., 2011. Comparison of multi-subject ICA methods for analysis of fMRI data. *Hum. Brain Map.* 32 (12), 2075–2095.
- Erus, G., Battapady, H., Satterthwaite, T.D., Hakonarson, H., Gur, R.E., Davatzikos, C., Gur, R.C., 2014. Imaging patterns of brain development and their relationship to cognition. *Cereb. Cortex*, <http://dx.doi.org/10.1093/cercor/bht425> (Epub ahead of print).
- Estrada, E., Higham, D.J., 2010. Network properties revealed through matrix functions. *SIAM Rev.* 52 (4), 696–714.
- Fair, D.A., Nigg, J.T., Iyer, S., Bathula, D., Mills, K.L., Dosenbach, N.U., Schlaggar, B.L., Mennes, M., Gutman, D., Bangaru, S., Buitelaar, J.K., Dickstein, D.P., Di Martino, A., Kennedy, D.N., Kelly, C., Luna, B., Schweitzer, J.B., Velanova, K., Wang, Y.F., Mostofsky, S., Castellanos, F.X., Milham, M.P., 2012. Distinct neural signatures detected for ADHD subtypes after controlling for micro-movements in resting state functional connectivity MRI data. *Front. Syst. Neurosci.* 6, 80.
- Feinberg, D.A., Moeller, S., Smith, S.M., Auerbach, E., Ramanna, S., Gunther, M., Glasser, M.F., Miller, K.L., Ugurbil, K., Yacoub, E., 2010. Multiplexed echo planar imaging for sub-second whole brain fMRI and fast diffusion imaging. *PLoS One* 5 (12), e15710.
- Filippini, N., MacIntosh, B.J., Hough, M.G., Goodwin, G.M., Frisoni, G.B., Smith, S.M., Matthews, P.M., Beckmann, C.F., Mackay, C.E., 2009. Distinct patterns of brain activity in young carriers of the APOE-epsilon4 allele. *Proc. Natl. Acad. Sci. U. S. A.* 106 (17), 7209–7214.
- Fischl, B., 2012. FreeSurfer. *Neuroimage* 62 (2), 774–781.
- Fornito, A., Bullmore, E.T., 2010. What can spontaneous fluctuations of the blood oxygenation-level-dependent signal tell us about psychiatric disorders? *Curr. Opin. Psychiatry* 23 (3), 239–249.
- Fox, M.D., Snyder, A.Z., Vincent, J.L., Corbetta, M., Van Essen, D.C., Raichle, M.E., 2005. The human brain is intrinsically organized into dynamic, anticorrelated functional networks. *Proc. Natl. Acad. Sci. U. S. A.* 102 (27), 9673–9678.
- Fox, M.D., Snyder, A.Z., Vincent, J.L., Raichle, M.E., 2007. Intrinsic fluctuations within cortical systems account for intertrial variability in human behavior. *Neuron* 56 (1), 171–184.
- Fox, M.D., Zhang, D., Snyder, A.Z., Raichle, M.E., 2009. The global signal and observed anticorrelated resting state brain networks. *J. Neurophysiol.* 101 (6), 3270–3283.
- Friston, K.J., 1994. Functional and effective connectivity in neuroimaging: a synthesis. *Hum. Brain Map.* 2 (1–2), 56–78.
- Friston, K.J., 2005. Models of brain function in neuroimaging. *Annu. Rev. Psychol.* 56, 57–87.
- Friston, K.J., 2009. Modalities, modes, and models in functional neuroimaging. *Science* 326 (5951), 399–403.
- Friston, K.J., 2011. Functional and effective connectivity: a review. *Brain Connect.* 1 (1), 13–36.
- Friston, K.J., Li, B., Daunizeau, J., Stephan, K.E., 2011. Network discovery with DCM. *Neuroimage* 56 (3), 1202–1221.
- Garrett, D.B., Kovacevic, N., McIntosh, A.R., Grady, C.L., 2011. The importance of being variable. *J. Neurosci.* 31 (12), 4496–4503.
- Garrett, D.D., Samanez-Larkin, G.R., MacDonald, S.W., Lindenberger, U., McIntosh, A.R., Grady, C.L., 2013. Moment-to-moment brain signal variability: a next frontier in human brain mapping? *Neurosci. Biobehav. Rev.* 37 (4), 610–624.
- Gerstner, W., Sprekeler, H., Deco, G., 2012. Theory and simulation in neuroscience. *Science* 338 (6103), 60–65.
- Glasser, M.F., Sotiroopoulos, S.N., Wilson, J.A., Coalson, T.S., Fischl, B., Andersson, J.L., Xu, J., Jbabdi, S., Webster, M., Polimeni, J.R., Van Essen, D.C., Jenkinson, M., Consortium, W.U.M.H., 2013. The minimal preprocessing pipelines for the Human Connectome Project. *Neuroimage* 80, 105–124.
- Gong, G., He, Y., Concha, L., Lebel, C., Gross, D.W., Evans, A.C., Beaulieu, C., 2009. Mapping anatomical connectivity patterns of human cerebral cortex using in vivo diffusion tensor imaging tractography. *Cereb. Cortex* 19 (3), 524–536.
- Greicius, M., 2008. Resting-state functional connectivity in neuropsychiatric disorders. *Curr. Opin. Neurol.* 21 (4), 424–430.
- Greicius, M.D., Krasnow, B., Reiss, A.L., Menon, V., 2003. Functional connectivity in the resting brain: a network analysis of the default mode hypothesis. *Proc. Natl. Acad. Sci. U. S. A.* 100 (1), 253–258.
- Greicius, M.D., Srivastava, G., Reiss, A.L., Menon, V., 2004. Default-mode network activity distinguishes Alzheimer's disease from healthy aging: evidence from functional MRI. *Proc. Natl. Acad. Sci. U. S. A.* 101 (13), 4637–4642.
- Greve, D.N., Fischl, B., 2009. Accurate and robust brain image alignment using boundary-based registration. *Neuroimage* 48 (1), 63–72.
- Guo, C.C., Kurth, F., Zhou, J., Mayer, E.A., Eickhoff, S.B., Kramer, J.H., Seeley, W.W., 2012. One-year test-retest reliability of intrinsic connectivity network fMRI in older adults. *Neuroimage* 61 (4), 1471–1483.
- Gur, R.C., Calkins, M.E., Satterthwaite, T.D., Ruparel, K., Bilker, W.B., Moore, T.M., Savitt, A.P., Hakonarson, H., Gur, R.E., 2014. Neurocognitive growth charting in psychosis spectrum youths. *JAMA Psychiatry* 71 (4), 366–374.
- Hagmann, P., Cammoun, L., Gigandet, X., Meuli, R., Honey, C.J., Wedeen, V.J., Sporns, O., 2008. Mapping the structural core of human cerebral cortex. *PLoS Biol.* 6 (7), e159.
- He, Y., Chen, Z.J., Evans, A.C., 2007. Small-world anatomical networks in the human brain revealed by cortical thickness from MRI. *Cereb. Cortex* 17 (10), 2407–2419.
- He, Y., Wang, J., Wang, L., Chen, Z.J., Yan, C., Yang, H., Tang, H., Zhu, C., Gong, Q., Zang, Y., Evans, A.C., 2009. Uncovering intrinsic modular organization of spontaneous brain activity in humans. *PLoS One* 4 (4), e5226.
- Hesselmann, G., Kell, C.A., Eger, E., Kleinschmidt, A., 2008. Spontaneous local variations in ongoing neural activity bias perceptual decisions. *Proc. Natl. Acad. Sci. U. S. A.* 105 (31), 10984–10989.
- van den Heuvel, M., Mandl, R., Hulshoff Pol, H., 2008. Normalized cut group clustering of resting-state fMRI data. *PLoS One* 3 (4), e2001.

- Hlinka, J., Palus, M., Vejmelka, M., Mantini, D., Corbetta, M., 2011. Functional connectivity in resting-state fMRI: is linear correlation sufficient? *Neuroimage* 54 (3), 2218–2225.
- Honey, C.J., Kotter, R., Breakspear, M., Sporns, O., 2007. Network structure of cerebral cortex shapes functional connectivity on multiple time scales. *Proc. Natl. Acad. Sci. U. S. A.* 104 (24), 10240–10245.
- Hu, S., Dai, G., Worrell, G.A., Dai, Q., Liang, H., 2011. Causality analysis of neural connectivity: critical examination of existing methods and advances of new methods. *IEEE Trans. Neural. Netw.* 22 (6), 829–844.
- Hutchison, R.M., Womelsdorf, T., Allen, E.A., Bandettini, P.A., Calhoun, V.D., Corbetta, M., Della Penna, S., Duyn, J.H., Glover, G.H., Gonzalez-Castillo, J., Handwerker, D.A., Keilholz, S., Kiviniemi, V., Leopold, D.A., de Pasquale, F., Sporns, O., Waller, M., Chang, C., 2013. Dynamic functional connectivity: promise, issues, and interpretations. *Neuroimage* 80, 360–378.
- Jenkinson, M., Beckmann, C.F., Behrens, T.E., Woolrich, M.W., Smith, S.M., 2012. *FSL Neuroimage* 62 (2), 782–790.
- Jiang, L., Xu, T., He, Y., Hou, X.H., Wang, J., Cao, X.Y., Wei, G.X., Yang, Z., He, Y., Zuo, X.N., 2014. Toward neurobiological characterization of functional homogeneity in the human cortex: regional variation, morphological association and functional covariance network organization. *Brain Struct. Funct.*, <http://dx.doi.org/10.1007/s00429-014-0795-8> (in press).
- Jiang, T., 2013. Brainnetome: a new -ome to understand the brain and its disorders. *Neuroimage* 80, 263–272.
- Jiang, T., Zhou, Y., Liu, B., Liu, Y., Song, M., 2013. Brainnetome-wide association studies in schizophrenia: the advances and future. *Neurosci. Biobehav. Rev.* 37 (10 Pt 2), 2818–2835.
- Jones, D.T., Vemuri, P., Murphy, M.C., Gunter, J.L., Senjem, M.L., Machulda, M.M., Przybelski, S.A., Gregg, B.E., Kantarci, K., Knopman, D.S., Boeve, B.F., Petersen, R.C., Jack, C.R.J., 2012. Non-stationarity in the resting brain's modular architecture. *PLoS One* 7 (6), e39731.
- Jordan, F., Liu, W.C., Davis, A.J., 2006. Topological keystone species: measures of positional importance in food webs. *Oikos* 112 (3), 535–546.
- Kandel, E.R., Markram, H., Matthews, P.M., Yuste, R., Koch, C., 2013. Neuroscience thinks big (and collaboratively). *Nat. Rev. Neurosci.* 14 (9), 659–664.
- Kannurpatti, S.S., Biswal, B.B., 2008. Detection and scaling of task-induced fMRI-BOLD response using resting state fluctuations. *Neuroimage* 40 (4), 1567–1574.
- Kapur, S., Phillips, A.G., Insel, T.R., 2012. Why has it taken so long for biological psychiatry to develop clinical tests and what to do about it? *Mol. Psychiatry* 17 (12), 1174–1179.
- Kelly, C., Biswal, B.B., Craddock, R.C., Castellanos, F.X., Milham, M.P., 2012. Characterizing variation in the functional connectome: promise and pitfalls. *Trends Cogn. Sci.* 16 (3), 181–188.
- Kiviniemi, V., Jauhainen, J., Tervonen, O., Paakko, E., Oikarinen, J., Vainionpaa, V., Rantala, H., Biswal, B., 2000. Slow vasomotor fluctuation in fMRI of anesthetized child brain. *Magn. Reson. Med.* 44 (3), 373–378.
- Kiviniemi, V., Kantola, J.H., Jauhainen, J., Hyvarinen, A., Tervonen, O., 2003. Independent component analysis of nondeterministic fMRI signal sources. *Neuroimage* 19 (2 Pt 1), 253–260.
- Landis, J.R., Koch, G.G., 1977. The measurement of observer agreement for categorical data. *Biometrics* 33 (1), 159–174.
- Lavoie-Courchesne, S., Rioux, P., Chouinard-Decorte, F., Sherif, T., Rousseau, M.E., Das, S., Adalat, R., Doyon, J., Craddock, C., Margulies, D., Chu, C., Lyttelton, O., Evans, A.C., Belloc, P., 2012. Integration of a neuroimaging processing pipeline into a pan-Canadian computing grid. In: High Performance Computing Symposium 2011.
- Leech, R., Sharp, D.J., 2014. The role of the posterior cingulate cortex in cognition and disease. *Brain* 137 (Pt 1), 12–32.
- Li, S.J., Li, Z., Wu, G., Zhang, M.J., Franczak, M., Antuono, P.G., 2002. Alzheimer disease: evaluation of a functional MR imaging index as a marker. *Radiology* 225 (1), 253–259.
- Liang, X., Zou, Q., He, Y., Yang, Y., 2013. Coupling of functional connectivity and regional cerebral blood flow reveals a physiological basis for network hubs of the human brain. *Proc. Natl. Acad. Sci. U. S. A.* 110 (5), 1929–1934.
- Liao, X.H., Xia, M.R., Xu, T., Dai, Z.J., Cao, X.Y., Niu, H.J., Zuo, X.N., Zang, Y.F., He, Y., 2013. Functional brain hubs and their test-retest reliability: a multiband resting-state functional MRI study. *Neuroimage* 83, 969–982.
- Lichtman, J.W., Denk, W., 2011. The big and the small: challenges of imaging the brain's circuits. *Science* 334 (6056), 618–623.
- Liu, C.Y., Krishnan, A.P., Yan, L., Smith, R.X., Kilroy, E., Alger, J.R., Ringman, J.M., Wang, D.J., 2013a. Complexity and synchronicity of resting state blood oxygenation level-dependent (BOLD) functional MRI in normal aging and cognitive decline. *J. Magn. Reson. Imaging* 38 (1), 36–45.
- Liu, D., Dong, Z., Zuo, X., Wang, J., Zang, Y., 2013b. Eyes-open/eyes-closed dataset sharing for reproducibility evaluation of resting state fMRI data analysis methods. *Neuroinformatics* 11 (4), 469–476.
- Mantzaris, A.V., Bassett, D.S., Wymbs, N.F., Estrada, E., Porter, M.A., Mucha, P.J., Grafton, S.T., Higham, D.J., 2013. Dynamic network centrality summarizes learning in the human brain. *J. Complex Netw.* 1 (1), 83–92.
- Marcus, D.S., Harms, M.P., Snyder, A.Z., Jenkinson, M., Wilson, J.A., Glasser, M.F., Barch, D.M., Archie, K.A., Burgess, G.C., Ramaratnam, M., Hodge, M., Horton, W., Herrick, R., Olsen, T., McKay, M., House, M., Hileman, M., Reid, E., Harwell, J., Coalson, T., Schindler, J., Elam, J.S., Curtiss, S.W., Van Essen, D.C., WU-MH, C., 2013. Human connectome project informatics: quality control, database services, and data visualization. *Neuroimage* 80, 202–219.
- Marcus, D.S., Harwell, J., Olsen, T., Hodge, M., Glasser, M.F., Prior, F., Jenkinson, M., Laumann, T., Curtiss, S.W., Van Essen, D.C., 2011. Informatics and data mining tools and strategies for the human connectome project. *Front. Neuroinform.* 5, 4.
- Marcus, D.S., Olsen, T.R., Ramaratnam, M., Buckner, R.L., 2007. The extensible neuroimaging archive toolkit: an informatics platform for managing, exploring, and sharing neuroimaging data. *Neuroinformatics* 5 (1), 11–34.
- Margulies, D.S., Bottger, J., Long, X., Lv, Y., Kelly, C., Schafer, A., Goldhahn, D., Abbush, A., Milham, M.P., Lohmann, G., Villringer, A., 2010. Resting developments: a review of fMRI post-processing methodologies for spontaneous brain activity. *MAGMA* 23 (5–6), 289–307.
- Markov, N.T., Ercsey-Ravasz, M., Van Essen, D.C., Knoblauch, K., Toroczkai, Z., Kennedy, H., 2013. Cortical high-density counterstream architectures. *Science* 342 (6158), 1238406.
- Markov, N.T., Ercsey-Ravasz, M.M., Ribeiro Gomes, A.R., Lamy, C., Magrou, L., Vezoli, J., Misery, P., Falchier, A., Quilodran, R., Gariel, M.A., Sallet, J., Gamanut, R., Huis-soud, C., Clavagnier, S., Giroud, P., Sappay-Marlinier, D., Barone, P., Dehay, C., Toroczkai, Z., Knoblauch, K., Van Essen, D.C., Kennedy, H., 2014. A weighted and directed interareal connectivity matrix for macaque cerebral cortex. *Cereb. Cortex* 24 (1), 17–36.
- Marsaglia, G., Tsang, W.W., Wang, J., 2003. Evaluating Kolmogorov's distribution. *J. Stat. Softw.* 8 (18), 1–4.
- Mason, M.F., Norton, M.I., Van Horn, J.D., Wegner, D.M., Grafton, S.T., Macrae, C.N., 2007. Wandering minds: the default network and stimulus-independent thought. *Science* 315 (5810), 393–395.
- Maxim, V., Sendur, L., Fadili, J., Suckling, J., Gould, R., Howard, R., Bullmore, E., 2005. Fractional gaussian noise, functional MRI and Alzheimer's disease. *Neuroimage* 25 (1), 141–158.
- McAvoy, M., Larson-Prior, L., Nolan, T.S., Vaishnavi, S.N., Raichle, M.E., d'Avossa, G., 2008. Resting states affect spontaneous BOLD oscillations in sensory and paralimbic cortex. *J. Neurophysiol.* 100 (2), 922–931.
- Mennes, M., Biswal, B.B., Castellanos, F.X., Milham, M.P., 2013. Making data sharing work: the FCP/INDI experience. *Neuroimage* 82, 683–691.
- Mennes, M., Zuo, X.N., Kelly, C., Di Martino, A., Zang, Y.F., Biswal, B., Castellanos, F.X., Milham, M.P., 2011. Linking inter-individual differences in neural activation and behavior to intrinsic brain dynamics. *Neuroimage* 54 (4), 2950–2959.
- Milham, M.P., 2012. Open neuroscience solutions for the connectome-wide association era. *Neuron* 73 (2), 214–218.
- Moeller, S., Yacoub, E., Olman, C.A., Auerbach, E., Strupp, J., Harel, N., Ugurbil, K., 2010. Multiband multislice GE-EPI at 7 Tesla, with 16-fold acceleration using partial parallel imaging with application to high spatial and temporal whole-brain fMRI. *Magn. Reson. Med.* 63 (5), 1144–1153.
- Mollov, E.K., Meyerand, M.E., Birn, R.M., 2014. The influence of spatial resolution and smoothing on the detectability of resting-state and task fMRI. *Neuroimage* 86, 221–230.
- Morgan, V.L., Rogers, B.P., Sonmezturk, H.H., Gore, J.C., Abou-Khalil, B., 2011. Cross hippocampal influence in mesial temporal lobe epilepsy measured with high temporal resolution functional magnetic resonance imaging. *Epilepsia* 52 (9), 1741–1749.
- Mowinckel, A.M., Espeseth, T., Westlye, L.T., 2012. Network-specific effects of age and in-scanner subject motion: a resting-state fMRI study of 238 healthy adults. *Neuroimage* 63 (3), 1364–1373.
- Muchinsky, P.M., 1996. The correction for attenuation. *Educ. Psychol. Measure.* 56 (1), 63–75.
- Mueller, S., Wang, D.H., Fox, M.D., Yeo, B.T.T., Sepulcre, J., Sabuncu, M.R., Shafee, R., Lu, J., Liu, H.S., 2013. Individual variability in functional connectivity architecture of the human brain. *Neuron* 77 (3), 586–595.
- Murphy, K., Birn, R.M., Bandettini, P.A., 2013. Resting-state fMRI confounds and cleanup. *Neuroimage* 80, 349–359.
- Murphy, K., Birn, R.M., Handwerker, D.A., Jones, T.B., Bandettini, P.A., 2009. The impact of global signal regression on resting state correlations: are anti-correlated networks introduced? *Neuroimage* 44 (3), 893–905.
- Nakagawa, S., Schielzeth, H., 2010. Repeatability for Gaussian and non-Gaussian data: a practical guide for biologists. *Biol. Rev. Camb. Philos. Soc.* 85 (4), 935–956.
- Nooner, K.B., Colcombe, S.J., Tobe, R.H., Mennes, M., Benedict, M.M., Moreno, A.L., Panek, L.J., Brown, S., Zavitz, S.T., Li, Q., Sikka, S., Gutman, D., Bangaru, S., Schlacter, R.T., Kamil, S.M., Anwar, A.R., Hinz, C.M., Kaplan, M.S., Rachlin, A.B., Adelsberg, S., Cheung, B., Khanuja, R., Yan, C., Craddock, C.C., Calhoun, V., Courtney, W., King, M., Wood, D., Cox, C.L., Kelly, A.M., Di Martino, A., Petkova, E., Reiss, P.T., Duan, N., Thomsen, D., Biswal, B., Coffey, B., Hoptman, M.J., Javitt, D.C., Pomara, N., Sridis, J.J., Koplowicz, H.S., Castellanos, F.X., Leventhal, B.L., Milham, M.P., 2012. The NKI-Rockland Sample: A model for accelerating the pace of discovery science in psychiatry. *Front. Neurosci.* 6, 152.
- Park, H.J., Friston, K., 2013. Structural and functional brain networks: from connections to cognition. *Science* 342 (6158), 1238411.
- Patriat, R., Molloy, E.K., Meier, T.B., Kirk, G.R., Nair, V.A., Meyerand, M.E., Prabhakaran, V., Birn, R.M., 2013. The effect of resting condition on resting-state fMRI reliability and consistency: a comparison between resting with eyes open, closed, and fixated. *Neuroimage* 78, 463–473.
- Pendse, G.V., Borsook, D., Becerra, L., 2011. A simple and objective method for reproducible resting state network (RSN) detection in fMRI. *PLoS One* 6 (12), e27594.
- Peng, Z.W., Xu, T., He, Q.H., Shi, C.Z., Wei, Z., Miao, G.D., Jing, J., Lim, K.O., Zuo, X.N., Chan, R.C., 2014. Default network connectivity as a vulnerability marker for obsessive compulsive disorder. *Psychol. Med.* 44, 1475–1484.

- Poppe, A.B., Wisner, K., Atluri, G., Lim, K.O., Kumar, V., Macdonald, A.W., 2013. Toward a neurometric foundation for probabilistic independent component analysis of fMRI data. *Cogn. Affect. Behav. Neurosci.* 13 (3), 641–659.
- Power, J.D., Barnes, K.A., Snyder, A.Z., Schlaggar, B.L., Petersen, S.E., 2012. Spurious but systematic correlations in functional connectivity MRI networks arise from subject motion. *Neuroimage* 59 (3), 2142–2154.
- Power, J.D., Barnes, K.A., Snyder, A.Z., Schlaggar, B.L., Petersen, S.E., 2013a. Steps toward optimizing motion artifact removal in functional connectivity MRI: a reply to carp. *Neuroimage* 76, 439–441.
- Power, J.D., Mitra, A., Laumann, T.O., Snyder, A.Z., Schlaggar, B.L., Petersen, S.E., 2014. Methods to detect, characterize, and remove motion artifact in resting state fMRI. *Neuroimage* 84, 320–341.
- Power, J.D., Schlaggar, B.L., Lessov-Schlaggar, C.N., Petersen, S.E., 2013b. Evidence for hubs in human functional brain networks. *Neuron* 79 (4), 798–813.
- Qi, X.Q., Fuller, E., Wu, Q., Wu, Y.Z., Zhang, C.Q., 2012. Laplacian centrality: a new centrality measure for weighted networks. *Inf. Sci.* 194, 240–253.
- Raichle, M.E., 2006. Neuroscience. the brain's dark energy. *Science* 314 (5803), 1249–1250.
- Raichle, M.E., MacLeod, A.M., Snyder, A.Z., Powers, W.J., Gusnard, D.A., Shulman, G.L., 2001. A default mode of brain function. *Proc. Natl. Acad. Sci. U.S.A.* 98 (2), 676–682.
- Raichle, M.E., Mintun, M.A., 2006. Brain work and brain imaging. *Annu. Rev. Neurosci.* 29, 449–476.
- Rubinov, M., Bullmore, E., 2013. Fledgling pathoconnectomics of psychiatric disorders. *Trends Cogn. Sci.* 17 (12), 641–647.
- Rubinov, M., Sporns, O., 2010. Complex network measures of brain connectivity: uses and interpretations. *Neuroimage* 52 (3), 1059–1069.
- Russell, J.F., 2013. If a job is worth doing, it is worth doing twice. *Nature* 496 (7443), 7447.
- Sadaghiani, S., Hesselmann, G., Friston, K.J., Kleinschmidt, A., 2010. The relation of ongoing brain activity, evoked neural responses, and cognition. *Front. Syst. Neurosci.* 4, 20.
- Salimi-Khorshidi, G., Douaud, G., Beckmann, C.F., Glasser, M.F., Griffanti, L., Smith, S.M., 2014. Automatic denoising of functional MRI data: combining independent component analysis and hierarchical fusion of classifiers. *Neuroimage* 90, 449–468.
- Salvador, R., Suckling, J., Coleman, M.R., Pickard, J.D., Menon, D., Bullmore, E., 2005. Neurophysiological architecture of functional magnetic resonance images of human brain. *Cereb. Cortex* 15 (9), 1332–1342.
- Satterthwaite, T.D., Elliott, M.A., Gerraty, R.T., Ruparel, K., Loughead, J., Calkins, M.E., Eickhoff, S.B., Hakonarson, H., Gur, R.C., Gur, R.E., Wolf, D.H., 2013. An improved framework for confound regression and filtering for control of motion artifact in the preprocessing of resting-state functional connectivity data. *Neuroimage* 64, 240–256.
- Satterthwaite, T.D., Elliott, M.A., Ruparel, K., Loughead, J., Prabhakaran, K., Calkins, M.E., Hopson, R., Jackson, C., Keefe, J., Riley, M., Mentch, F.D., Sleiman, P., Verma, R., Davatzikos, C., Hakonarson, H., Gur, R.C., Gur, R.E., 2014. Neuroimaging of the philadelphia neurodevelopmental cohort. *Neuroimage* 86, 544–553.
- Satterthwaite, T.D., Wolf, D.H., Loughead, J., Ruparel, K., Elliott, M.A., Hakonarson, H., Gur, R.C., Gur, R.E., 2012. Impact of in-scanner head motion on multiple measures of functional connectivity: relevance for studies of neurodevelopment in youth. *Neuroimage* 60 (1), 623–632.
- Shehzad, Z., Kelly, A.M., Reiss, P.T., Gee, D.G., Gotimer, K., Uddin, L.Q., Lee, S.H., Margulies, D.S., Roy, A.K., Biswal, B.B., Petkova, E., Castellanos, F.X., Milham, M.P., 2009. The resting brain: unconstrained yet reliable. *Cereb. Cortex* 19 (10), 2209–2229.
- Shou, H., Eloyan, A., Lee, S., Zipunnikov, V., Crainiceanu, A.N., Nebel, M.B., Caffo, B., Lindquist, M.A., Crainiceanu, C.M., 2014. Quantifying the reliability of image replication studies: the image intraclass correlation coefficient (I2C2). *Cogn. Affect. Behav. Neurosci.* 13 (4), 714–724.
- Shroud, P.E., Fleiss, J.L., 1979. Intraclass correlations: uses in assessing rater reliability. *Psychol. Bull.* 86 (2), 420–428.
- Shulman, G.L., Fiez, J.A., Corbetta, M., Buckner, R.L., Miezin, F.M., Raichle, M.E., Petersen, S.E., 1997. Common blood flow changes across visual tasks. II. Decreases in cerebral cortex. *J. Cogn. Neurosci.* 9 (5), 648–663.
- Singh, I., Rose, N., 2009. Biomarkers in psychiatry. *Nature* 460 (7252), 202–207.
- Smith, R.X., Yan, L., Wang, D.J., 2014. Multiple time scale complexity analysis of resting state fMRI. *Brain Imaging Behav.* 8 (2), 284–291.
- Smith, S.M., Beckmann, C.F., Andersson, J., Auerbach, E.J., Bijsterbosch, J., Douaud, G., Duff, E., Feinberg, D.A., Griffanti, L., Harms, M.P., Kelly, M., Laumann, T., Miller, K.L., Moeller, S., Petersen, S., Power, J., Salimi-Khorshidi, G., Snyder, A.Z., Vu, A.T., Woolrich, M.W., Xu, J., Yacoub, E., Ugurbil, K., Van Essen, D.C., Glasser, M.F., Consortium, W.U.M.H., 2013a. Resting-state fMRI in the Human Connectome Project. *Neuroimage* 80, 144–168.
- Smith, S.M., Miller, K.L., Salimi-Khorshidi, G., Webster, M., Beckmann, C.F., Nichols, T.E., Ramsey, J.D., Woolrich, M.W., 2011. Network modelling methods for fMRI. *Neuroimage* 54 (2), 875–891.
- Smith, S.M., Vidaurre, D., Beckmann, C.F., Glasser, M.F., Jenkinson, M., Miller, K.L., Nichols, T.E., Robinson, E.C., Salimi-Khorshidi, G., Woolrich, M.W., Barch, D.M., Ugurbil, K., Van Essen, D.C., 2013b. Functional connectomics from resting-state fMRI. *Trends Cogn. Sci.* 17 (12), 666–682.
- Song, J., Deshpande, A.S., Meier, T.B., Tudorascu, D.L., Vergun, S., Nair, V.A., Biswal, B.B., Meyerand, M.E., Birn, R.M., Bellec, P., Prabhakaran, V., 2012. Age-related differences in test-retest reliability in resting-state brain functional connectivity. *PLoS One* 7 (12), e49847.
- Song, X.W., Dong, Z.Y., Long, X.Y., Li, S.F., Zuo, X.N., Zhu, C.Z., He, Y., Yan, C.G., Zang, Y.F., 2011. REST: a toolkit for resting-state functional magnetic resonance imaging data processing. *PLoS One* 6 (9), e25031.
- Sporns, O., 2013. The human connectome: origins and challenges. *Neuroimage* 80, 53–61.
- Sporns, O., Tononi, G., Edelman, G.M., 2000. Theoretical neuroanatomy: relating anatomical and functional connectivity in graphs and cortical connection matrices. *Cereb. Cortex* 10 (2), 127–141.
- Sporns, O., Tononi, G., Kotter, R., 2005. The human connectome: a structural description of the human brain. *PLoS Comput. Biol.* 1 (4), e42.
- Stark, D.E., Margulies, D.S., Shehzad, Z.E., Reiss, P., Kelly, A.M., Uddin, L.Q., Gee, D.G., Roy, A.K., Banich, M.T., Castellanos, F.X., Milham, M.P., 2008. Regional variation in interhemispheric coordination of intrinsic hemodynamic fluctuations. *J. Neurosci.* 28 (51), 13754–13764.
- Stephan, K.E., Friston, K.J., 2010. Analyzing effective connectivity with fMRI. *Wiley Interdiscip. Rev. Cogn. Sci.* 1 (3), 446–459.
- Thomason, M.E., Dennis, E.L., Joshi, A.A., Joshi, S.H., Dinov, I.D., Chang, C., Henry, M.L., Johnson, R.F., Thompson, P.M., Toga, A.W., Glover, G.H., Van Horn, J.D., Gotlib, I.H., 2011. Resting-state fMRI can reliably map neural networks in children. *Neuroimage* 55 (1), 165–175.
- Tian, L., Ren, J., Zang, Y., 2012. Regional homogeneity of resting state fMRI signals predicts stop signal task performance. *Neuroimage* 60 (1), 539–544.
- Tomasi, D., Volkow, N.D., 2010. Functional connectivity density mapping. *Proc. Natl. Acad. Sci. U.S.A.* 107 (21), 9885–9890.
- Tomasi, D., Volkow, N.D., 2012. Aging and functional brain networks. *Mol. Psychiatry* 17 (5), 471–479.
- Tomasi, D., Wang, G.J., Volkow, N.D., 2013. Energetic cost of brain functional connectivity. *Proc. Natl. Acad. Sci. U.S.A.* 110 (33), 13642–13647.
- Tononi, G., Sporns, O., Edelman, G.M., 1994. A measure for brain complexity: relating functional segregation and integration in the nervous system. *Proc. Natl. Acad. Sci. U.S.A.* 91 (11), 5033–5037.
- Turk-Browne, N.B., 2013. Functional interactions as big data in the human brain. *Science* 342 (6158), 580–584.
- Tyszka, J.M., Kennedy, D.P., Paul, L.K., Adolphs, R., 2013. Largely typical patterns of resting-state functional connectivity in high-functioning adults with autism. *Cereb. Cortex*, <http://dx.doi.org/10.1093/cercor/bht040> (Epub ahead of print).
- Uddin, L.Q., Kelly, A.M., Biswal, B.B., Margulies, D.S., Shehzad, Z., Shaw, D., Ghafari, M., Rotrosen, J., Adler, L.A., Castellanos, F.X., Milham, M.P., 2008. Network homogeneity reveals decreased integrity of default-mode network in ADHD. *J. Neurosci. Methods* 169 (1), 249–254.
- Van Dijk, K.R., Hedden, T., Venkataraman, A., Evans, K.C., Lazar, S.W., Buckner, R.L., 2010. Intrinsic functional connectivity as a tool for human connectomics: theory, properties, and optimization. *J. Neurophysiol.* 103 (1), 297–321.
- Van Dijk, K.R., Sabuncu, M.R., Buckner, R.L., 2012. The influence of head motion on intrinsic functional connectivity MRI. *Neuroimage* 59 (1), 431–438.
- Van Essen, D.C., 2012. Cortical cartography and Caret software. *Neuroimage* 62 (2), 757–764.
- Van Essen, D.C., Dierker, D.L., 2007. Surface-based and probabilistic atlases of primate cerebral cortex. *Neuron* 56 (2), 209–225.
- Van Essen, D.C., Glasser, M.F., Dierker, D.L., Harwell, J., Coalson, T., 2012. Parcellations and hemispheric asymmetries of human cerebral cortex analyzed on surface-based atlases. *Cereb. Cortex* 22 (10), 2241–2262.
- Van Essen, D.C., Smith, S.M., Barch, D.M., Behrens, T.E., Yacoub, E., Ugurbil, K., Consortium, W.U.M.H., 2013. The WU-Minn Human Connectome Project: an overview. *Neuroimage* 80, 62–79.
- Wang, J., Zuo, X., Dai, Z., Xia, M., Zhao, Z., Zhao, X., Jia, J., Han, Y., He, Y., 2013a. Disrupted functional brain connectome in individuals at risk for Alzheimer's disease. *Biol. Psychiatry* 73 (5), 472–481.
- Wang, J., Zuo, X., He, Y., 2010. Graph-based network analysis of resting-state functional MRI. *Front. Syst. Neurosci.* 4, 16.
- Wang, T., Chen, Z., Zhao, G., Hitchman, G., Liu, C., Zhao, X., Liu, Y., Chen, A., 2014. Linking inter-individual differences in the conflict adaptation effect to spontaneous brain activity. *Neuroimage* 90C, 146–152.
- Wang, Y., Du, H., Xia, M., Ren, L., Xu, M., Xie, T., Gong, G., Xu, N., Yang, H., He, Y., 2013. A hybrid CPU-GPU accelerated framework for fast mapping of high-resolution human brain connectome. *PLoS One* 8 (5), e62789.
- Wei, G.X., Dong, H.M., Yang, Z., Luo, J.M., Zuo, X.N., 2014. Tai chi chuan optimizes the functional organization of the intrinsic human brain architecture in older adults. *Front. Aging Neurosci.* 8, 74.
- Wei, G.X., Xu, T., Fan, F.M., Dong, H.M., Jiang, L.L., Li, H.J., Yang, Z., Luo, J., Zuo, X.N., 2013. Can tai chi reshape the brain? A brain morphometry study. *PLoS One* 8 (4), e61038.
- Wig, G.S., Laumann, T.O., Cohen, A.L., Power, J.D., Nelson, S.M., Glasser, M.F., Miezin, F.M., Snyder, A.Z., Schlaggar, B.L., Petersen, S.E., 2013. Parcellating an individual subject's cortical and subcortical brain structures using Snowball Sampling of resting-state correlations. *Cereb. Cortex*, <http://dx.doi.org/10.1093/cercor/bht056> (Epub ahead of print).
- Wink, A.M., Bullmore, E., Barnes, A., Bernard, F., Suckling, J., 2008. Monofractal and multifractal dynamics of low frequency endogenous brain oscillations in functional MRI. *Hum. Brain Map.* 29 (7), 791–801.

- Wu, T., Zang, Y.F., Wang, L., Long, X.Y., Li, K.C., Chan, P., 2007. Normal aging decreases regional homogeneity of the motor areas in the resting state. *Neurosci. Lett.* 423 (3), 189–193.
- Xie, X., Cao, Z., Weng, X., 2008. Spatiotemporal nonlinearity in resting-state fMRI of the human brain. *Neuroimage* 40 (4), 1672–1685.
- Xing, X.X., Xu, T., Yang, Z., Zuo, X.N., 2013. Non-local Means Smoothing: A Demonstration on Multiband Resting State MRI. In: Poster (No. 2038) presented at 19th Annual Meeting of the Organization for Human Brain Mapping (OHBM), June 16–20, Washington State Convention Center in Seattle, USA.
- Xu, P., Huang, R., Wang, J., Van Dam, N.T., Xie, T., Dong, Z., Chen, C., Gu, R., Zang, Y.F., He, Y., Fan, J., Luo, Y., 2014. Different topological organization of human brain functional networks with eyes open versus eyes closed. *Neuroimage* 90, 246–255.
- Yan, C., Liu, D., He, Y., Zou, Q., Zhu, C., Zuo, X., Long, X., Zang, Y., 2009. Spontaneous brain activity in the default mode network is sensitive to different resting-state conditions with limited cognitive load. *PLoS One* 4 (5), e5743.
- Yan, C.G., Cheung, B., Kelly, C., Colcombe, S., Craddock, R.C., Di Martino, A., Li, Q., Zuo, X.N., Castellanos, F.X., Milham, M.P., 2013a. A comprehensive assessment of regional variation in the impact of head micromovements on functional connectomics. *Neuroimage* 76, 183–201.
- Yan, C.G., Craddock, R.C., Zuo, X.N., Zang, Y.F., Milham, M.P., 2013b. Standardizing the intrinsic brain: towards robust measurement of inter-individual variation in 1000 functional connectomes. *Neuroimage* 80, 246–262.
- Yan, C.G., Zang, Y.F., 2010. DPARSF: A MATLAB toolbox for 'Pipeline' data analysis of resting-state fMRI. *Front. Syst. Neurosci.* 4, 13.
- Yang, H., Long, X.Y., Yang, Y., Yan, H., Zhu, C.Z., Zhou, X.P., Zang, Y.F., Gong, Q.Y., 2007. Amplitude of low frequency fluctuation within visual areas revealed by resting-state functional MRI. *Neuroimage* 36 (1), 144–152.
- Yang, Z., Chang, C., Xu, T., Jiang, L., Handwerker, D.A., Castellanos, F.X., Milham, M.P., Bandettini, P.A., Zuo, X.N., 2014. Connectivity trajectory across lifespan differentiates the precuneus from the default network. *Neuroimage* 89C, 45–56.
- Yang, Z., LaConte, S., Weng, X., Hu, X., 2008. Ranking and averaging independent component analysis by reproducibility (RAICAR). *Hum. Brain Map.* 29 (6), 711–725.
- Yang, Z., Zuo, X.N., Wang, P., Li, Z., LaConte, S.M., Bandettini, P.A., Hu, X.P., 2012. Generalized RAICAR: discover homogeneous subject (sub)groups by reproducibility of their intrinsic connectivity networks. *Neuroimage* 63 (1), 403–414.
- Yeo, B.T., Krienen, F.M., Chee, M.W., Buckner, R.L., 2013. Estimates of segregation and overlap of functional connectivity networks in the human cerebral cortex. *Neuroimage* 88C, 212–227.
- Yeo, B.T., Krienen, F.M., Sepulcre, J., Sabuncu, M.R., Lashkari, D., Hollinshead, M., Roffman, J.L., Smoller, J.W., Zollei, L., Polimeni, J.R., Fischl, B., Liu, H., Buckner, R.L., 2011. The organization of the human cerebral cortex estimated by intrinsic functional connectivity. *J. Neurophysiol.* 106 (3), 1125–1165.
- Zador, A.M., Dubnau, J., Oyibo, H.K., Zhan, H., Cao, G., Peikon, I.D., 2012. Sequencing the connectome. *PLoS Biol.* 10 (10), e1001411.
- Zang, Y., Jiang, T., Lu, Y., He, Y., Tian, L., 2004. Regional homogeneity approach to fMRI data analysis. *Neuroimage* 22 (1), 394–400.
- Zang, Y.F., He, Y., Zhu, C.Z., Cao, Q.J., Sui, M.Q., Liang, M., Tian, L.X., Jiang, T.Z., Wang, Y.F., 2007. Altered baseline brain activity in children with ADHD revealed by resting-state functional MRI. *Brain Dev.* 29 (2), 83–91.
- Zhang, D., Raichle, M.E., 2010. Disease and the brain's dark energy. *Nat. Rev. Neurol.* 6 (1), 15–28.
- Zhao, K., Yan, W.J., Chen, Y.H., Zuo, X.N., Fu, X., 2013. Amygdala volume predicts inter-individual differences in fearful face recognition. *PLoS One* 8 (8), e74096.
- Zhong, Y., Wang, H., Lu, G., Zhang, Z., Jiao, Q., Liu, Y., 2009. Detecting functional connectivity in fMRI using PCA and regression analysis. *Brain Topogr.* 22 (2), 134–144.
- Zhu, L., Fan, Y., Zou, Q., Wang, J., Gao, J.H., Niu, Z., 2014. Temporal reliability and lateralization of the resting-state language network. *PLoS One* 9 (1), e85880.
- Zou, Q., Long, X., Zuo, X., Yan, C., Zhu, C., Yang, Y., Liu, D., He, Y., Zang, Y., 2009. Functional connectivity between the thalamus and visual cortex under eyes closed and eyes open conditions: a resting-state fMRI study. *Hum. Brain Map.* 30 (9), 3066–3078.
- Zou, Q., Ross, T.J., Gu, H., Geng, X., Zuo, X.N., Hong, L.E., Gao, J.H., Stein, E.A., Zang, Y.F., Yang, Y., 2013. Intrinsic resting-state activity predicts working memory brain activation and behavioral performance. *Hum. Brain Map.* 34 (12), 3204–3215.
- Zou, Q.H., Zhu, C.Z., Yang, Y., Zuo, X.N., Long, X.Y., Cao, Q.J., Wang, Y.F., Zang, Y.F., 2008. An improved approach to detection of amplitude of low-frequency fluctuation (ALFF) for resting-state fMRI: fractional ALFF. *J. Neurosci. Methods* 172 (1), 137–141.
- Zuo, X.N., Di Martino, A., Kelly, C., Shehzad, Z.E., Gee, D.G., Klein, D.F., Castellanos, F.X., Biswal, B.B., Milham, M.P., 2010a. The oscillating brain: complex and reliable. *Neuroimage* 49 (2), 1432–1445.
- Zuo, X.N., Ehmke, R., Mennes, M., Imperati, D., Castellanos, F.X., Sporns, O., Milham, M.P., 2012. Network centrality in the human functional connectome. *Cereb. Cortex* 22 (8), 1862–1875.
- Zuo, X.N., Kelly, C., Adelstein, J.S., Klein, D.F., Castellanos, F.X., Milham, M.P., 2010b. Reliable intrinsic connectivity networks: test-retest evaluation using ICA and dual regression approach. *Neuroimage* 49 (3), 2163–2177.
- Zuo, X.N., Kelly, C., Di Martino, A., Mennes, M., Margulies, D.S., Bangaru, S., Grzadzinski, R., Evans, A.C., Zang, Y.F., Castellanos, F.X., Milham, M.P., 2010c. Growing together and growing apart: regional and sex differences in the lifespan developmental trajectories of functional homotopy. *J. Neurosci.* 30 (45), 15034–15043.
- Zuo, X.N., Xing, X.X., 2011. Effects of non-local diffusion on structural mri preprocessing and default network mapping: statistical comparisons with isotropic/anisotropic diffusion. *PLoS One* 6 (10), e26703.
- Zuo, X.N., Xu, T., Jiang, L., Yang, Z., Cao, X.Y., He, Y., Zang, Y.F., Castellanos, F.X., Milham, M.P., 2013. Toward reliable characterization of functional homogeneity in the human brain: preprocessing, scan duration, imaging resolution and computational space. *Neuroimage* 65, 374–386.